SC5005.46FR

NASA CR-145161

DEVELOPMENT OF AN (AlGaAs-GaAs) GRADED BANDGAP SOLAR CELL

by

R. Sahai and J. S. Harris, Jr.

December 1976

Prepared under Contract No. NAS1-13548

by

Rockwell International/Science Center

1049 Camino Dos Rios

Thousand Oaks, California 91360

Approved for public release; distribution unlimited

REPORT DOCUMENTATION PAGE

READ INSTRUCTIONS BEFORE COMPLETING FORM

1. REPORT NUMBER

2. GOVT ACCESSION NO.

3. RECIPIENT'S CATALOG NUMBER

4. TITLE (and Subtitle)
Development of an Aluminum-Gallium-Arsenide-Gallium Arsenide (AlGaAs-GaAs) Graded Band Gap Solar Cell

5. TYPE OF REPORT & PERIOD COVERED
Final Report for period 10-23-74 thru 10-01-76

6. PERFORMING ORG. REPORT NUMBER
SC5005.46FR

7. AUTHOR(s)
Raj Sahai
James S. Harris, Jr.

8. CONTRACT OR GRANT NUMBER(s)
NAS1-13548

9. PERFORMING ORGANIZATION NAME AND ADDRESS
Rockwell International/Science Center
1049 Camino Dos Rios
Thousand Oaks, California 91360

10. PROGRAM ELEMENT, PROJECT, TASK AREA & WORK UNIT NUMBERS

11. CONTROLLING OFFICE NAME AND ADDRESS
NASA/Langley Research Center
Hampton, Virginia 20771

12. REPORT DATE
December 1976

13. NUMBER OF PAGES
59 pages

14. MONITORING AGENCY NAME & ADDRESS(if different from Controlling Office)

15. SECURITY CLASS. (of this report)
UNCLASSIFIED

15a. DECLASSIFICATION/DOWNGRADING SCHEDULE

16. DISTRIBUTION STATEMENT (of this Report)

Approved for public release; distribution unlimited

17. DISTRIBUTION STATEMENT (of the abstract entered in Block 20, if different from Report)

18. SUPPLEMENTARY NOTES

19. KEY WORDS (Continue on reverse side if necessary and identify by block number)

Heterojunction, Graded Bandgap, Solar Cell, GaAs.

20. ABSTRACT (Continue on reverse side if necessary and identify by block number)

GaAs based solar cells have the potential to achieve greater than 20% AMO conversion efficiency if the effect of a high surface recombination velocity at the GaAs surface can be overcome. One means to overcome this loss is the utilization of a built-in electric field created by compositional grading in the GaAlAs layer of a GaAlAs/GaAs solar cell. The results of an experimental program to develop the epitaxial growth techniques and analytical characterization techniques to fabricate graded bandgap solar cells are reported.

FOREWORD

This report was prepared by Rockwell International, Science Center under contract NAS1-13548. This report covers the period of 23 October 1974 through 1 October 1976, and is the Final Report on this contract. The work described herein was carried out by the Rockwell International, Science Center, Thousand Oaks, California.

The principal investigator for this project was Dr. Raj Sahai. The principal technical support for this work at the Science Center was provided by Dennis D. Edwall, Earl S. Cory and Imre S. Santha.

The program manager was Dr. James S. Harris, Jr.

The technical officer for this project from NASA/Langley Research Center was James A. Hutchby.

ABSTRACT

GaAs based solar cells have the potential to achieve greater than 20% AMO conversion efficiency if the effect of a high surface recombination velocity at the GaAs surface can be overcome. One means to overcome this loss is the utilization of a built-in electric field created by compositional grading in the GaAlAs layer of a GaAlAs/GaAs solar cell. The results of an experimental program to develop the epitaxial growth techniques and analytical characterization techniques to fabricate graded bandgap solar cells are reported.

TABLE OF CONTENTS

LIST OF ILLUSTRATIONS

LIST OF ILLUSTRATIONS (Cont.)

LIST OF ILLUSTRATIONS (Cont.)

1.0 INTRODUCTION AND SUMMARY

NASA presently utilizes a large number of 10-12% AMO efficiency solar cells to provide primary electrical power aboard nearly all of their spacecraft. The solar cell portion of the total power system cost "in orbit" is quite high because the solar panels are relatively heavy which greatly increases the orbiting cost. It has been estimated that by improving solar cell efficiency up to 20%, there is a potential savings in excess of $100 million for cells required in space missions for the next decade.[1] The development of such high efficiency cells would have a major impact on both future mission costs and the increased magnitude of available power one could achieve.

GaAs based solar cells have the potential to achieve greater than 20% AMO conversion efficiency.[2] Progress toward realizing this goal has, however, been very slow. The major limitation to realizing this high theoretical efficiency has been the high surface recombination velocity of GaAs which results in a high recombination loss of photogenerated electrons and holes at the GaAs surface. The GaAlAs/GaAs heteroface cell was the first development to greatly reduce this problem. The heteroface cell utilizes a GaAlAs window layer so that the high loss GaAs surface is replaced by a low loss p-p GaAlAs/GaAs heterojunction interface. The efficiency of these cells is then only limited by the collection of photogenerated carriers in the wide bandgap GaAlAs layer.

One means to improve collection of minority carriers in the GaAlAs layer is to utilize a built-in electric field to add a drift component to the transport of carriers toward the p-n junction. One method of creating this field is through compositional grading of the $Ga_{(1-x)}Al_xAs$ layer such that $x = 0$ at the p-n junction and increases toward unity ($x = 1$) at the surface. Graded bandgap cells with this alloy system were first described by Hutchby.[3] An energy band diagram for a p on n graded bandgap solar cell is shown in Fig. 1. The improved carrier collection (for electrons) results from the electric field created by the gradient in the conduction band created by composition grading in the GaAlAs layer. The built-in field can be sufficiently high to completely overcome carrier transport to the high loss surface and near

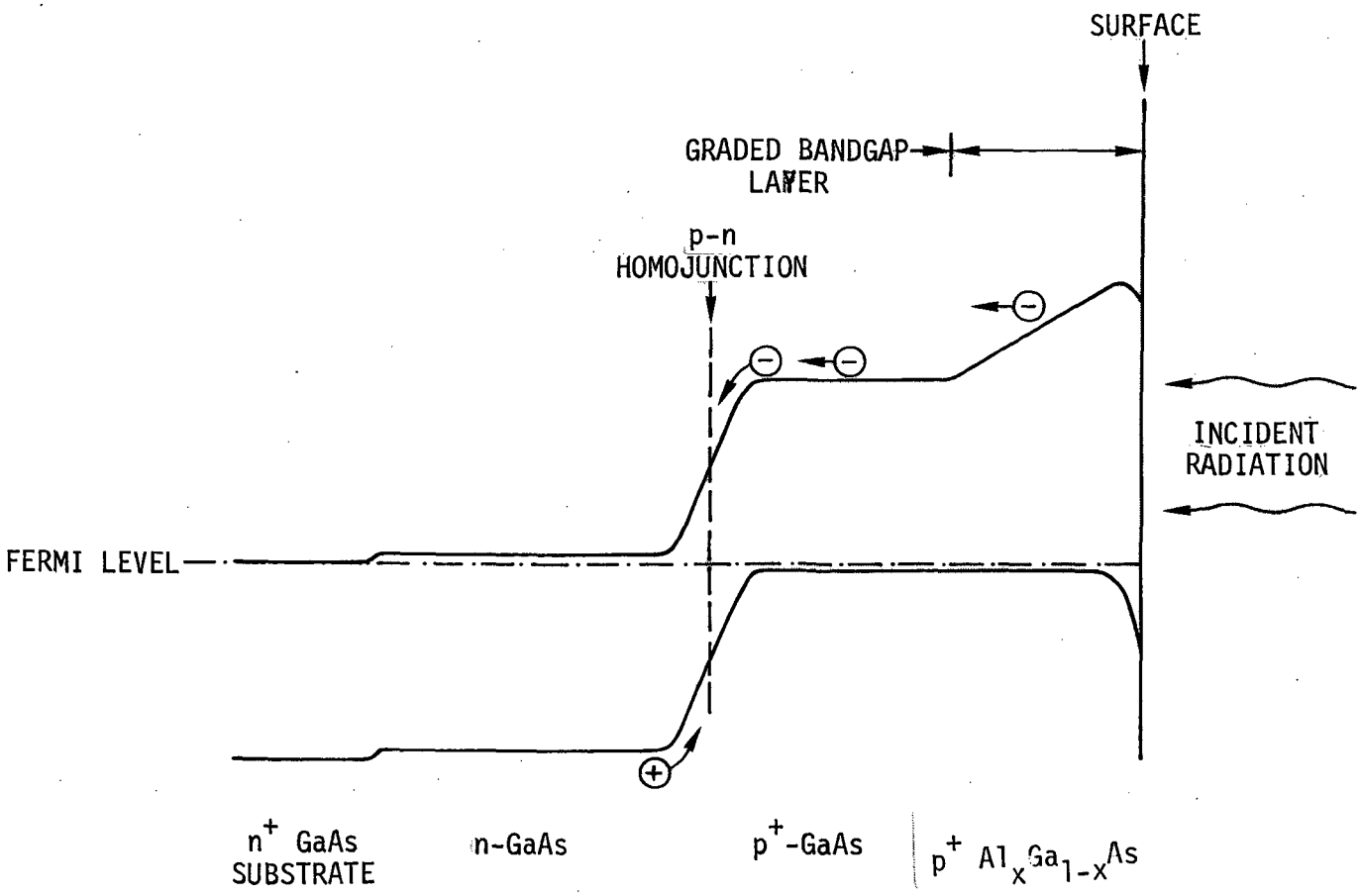

Fig. 1 Energy-band diagram for a p/n GaAlAs/GaAs graded bandgap heteroface solar cell. The graded bandgap region near the surface increases electron collection due to the built-in electric field for minority carriers (electrons).

theoretical efficiencies in excess of 20% are predicted.

In this research program, we have emphasized the development of liquid phase epitaxial (LPE) techniques to grow a graded composition layer and analytical techniques to experimentally characterize both the electrical and chemical properties of these graded layers. The LPE growth utilized melt mixing to produce a graded composition GaAlAs layer. Composition vs. depth profiles were measured by high resolution SEM-X-ray analysis, proton Rutherford backscattering and Auger electron spectroscopy combined with sputtering for thin layer removal. These techniques proved adequate to characterize the graded layers.

Solar cells fabricated from these graded composition structures demonstrated an enhanced photoresponse at short wavelengths compared to similarly fabricated, non-graded structures. One of the problems in realizing these structures is that the compositional grading must be monotonically increasing all the way out to the surface. This proved to be very difficult to achieve over large areas and with any degree of reproducibility by the melt mixing LPE technique. Thus, while the graded bandgap concept still appears to be a viable candidate to achieve high efficiency solar conversion, it does not appear that this structure can be realized by LPE techniques. Recent developments in improving molecular beam epitaxy (MBE) make this a very attractive growth system to pursue the development of a graded bandgap solar cell.

2.0 PROGRAM GOALS AND APPROACH

2.1 GOALS

The theoretical limit for the GaAs solar cell efficiency is 25% as compared to about 20% for Si solar cells. The principal reason for the relatively low efficiencies of the practical GaAs solar cells is the simultaneous occurance of extremely large optical absorption coefficients and large surface recombination velocity. Several approaches have been suggested to overcome this limitation in GaAs. Sahai and Milnes[4] showed that by using a heterojunction approach that utilizes a ZnSe window region, the ZnSe-GaAs pair can result in a practical efficiency value in the 13-16% range. Ellis and Moss[5] calculated that GaAs solar cell efficiency could be raised above 20% by incorporating a built-in electric field for compensating the high surface recombination velocity effect. They suggested an exponential doping profile in the surface layer. Tsaur et al.[6] showed that the practical Zn-diffusion profiles are far from the ideal exponential profile and do not provide the surface electric field for solving the high surface recombination velocity problem. Vaidyanathan and Walker[7] have demonstrated that near exponential impurity profiles can be obtained in GaAs solar cells by ion implantation. However, the spectral response of such cells showed only a small collection from the surface region indicating that the implantation damage near the surface is not annealed out.

Near the beginning of this program, the GaAlAs/GaAs heteroface cells had already demonstrated improved solar energy conversion efficiency (Hovel and Woodall[8]). However, in the heteroface approach the optical absorption near the surface is still lost. The overall goal of this program was to demonstrate the technical feasibility of utilizing a concentration gradient of Al in the active GaAlAs region to increase the efficiency of GaAlAs/GaAs solar cells above the then state of the art value of 13.5% at air mass zero (AM0). This was subdivided into the following tasks:

(1) Develop a LPE Growth Technique which results in the desired compositional grading from the theoretical calculations done by Hutchby[3,9-11], the optimum grading parameters

were to change x in $Ga_{1-x}Al_xAs$ from zero at the interface to ~0.35 at the surface over a 0.7μm distance.

(2) Develop an Analytical Technique to obtain the depth vs. composition profile of the graded GaAlAs layer.

(3) Optimize the cell design to improve the energy conversion efficiency.

2.2 APPROACH

2.2.1 Graded GaAlAs Layer Growth

The growth technique to obtain the thin graded GaAlAs layer is the most critical task in the fabrication of the proposed solar cell structure. GaAlAs layers have been prepared by a number of techniques. The growth technique suitable for this structure must meet the following requirements:

1) It should be capable of growing uniform thickness sub-micron layers.
2) It should be capable of growing $Ga_xAl_{1-x}As$ in the composition range between x = 1 and x = 0.1.
3) The growth process should allow controlled variation of composition and doping during growth.
4) The grown layers should be of high electrical and optical quality.

The growth techniques available to grow GaAlAs layers are (A) iodine-vapor disproportionation[12] transport, (B) liquid phase epitaxy from Ga solution[13] and (C) pyrolytic decomposition of metal-organic compounds[14] in a chemical vapor deposition system. The technique A can meet the first and fourth requirements but cannot provide the controlled grading and does not cover the whole composition range of interest. The technique C can meet the first three requirements but does not yield good quality layers. The LPE technique B meets the first, second and fourth requirements. In view of the fact that LPE technique has resulted in great improvements in a number of opto-electronic devices, our approach was to work on this technique to fabricate the GaAlAs/GaAs graded heterojunction solar cell.

An important feature of Ga-Al-As system is the large distribution coefficient of aluminum[15] between the solid and liquid phases in dilute solutions (Ga-rich). This fact can be utilized in conjunction with the technique of using thin-melts. The rapid depletion of Al from the liquid phase will produce a decreasing Al content in the grown layer and thus provide the composition grading. However, the grading obtained by this technique is the inverse of that needed for the solar cell. In addition to this problem, a quick calculation of the required melt thickness, based on the design parameters for the GaAlAs layer, viz. 0.7 micron thickness and grading from ∿35% Al to 0% Al concentration, results in non-practical melt thicknesses (of the order of 2 mils) even at low growth temperatures. The minimum practical melt thickness is about an order of magnitude larger at 20 mils (0.5 mm).

We, therefore, proposed an alternative technique to obtain the composition grading by LPE process. Based on our extensive work on LPE growth of several 3-5 compounds, we have established[16] that in systems where complete solid solubility exists between two materials, when a layer of one material is grown on the other material, the interface consists of a continuously graded region from one composition to the other. The transient processes coupled with the finite diffusion coefficients of the elements in the solution provide this grading. Under normal growth conditions, for the GaAs-GaAlAs system, this grading length is estimated to be less than or of the order of 300Å. Our approach to increase this grading distance was to introduce intentional melt-mixing to prolong the initial non-equilibrium state. The details of this process are discussed in section 3.1.

2.2.2 Composition Profiling of the GaAlAs Layer

The other important aspect of this program was to investigate various techniques for evaluating the composition grading of the GaAlAs surface layer. Our goal was to develop one reliable and non-destructive technique for composition profiling and another technique, which may be destructive in nature, for comparison and to increase the confidence level of the quantitative analysis.

Since we are interested in the depth profile of the GaAlAs layer composition, the non-destructive techniques require absorption or reflection type measurements on the sample and then the measured data can be deconvolved to provide the composition vs. depth profile. Optical measurements are simple to handle and at our laboratory we already had developed a profiling technique[17] using the optical transmission. However, this technique can be used for thin films, only if the substrate is optically transparent in the wavelength range where the thin film is optically absortive, viz. it can be used for thin films with bandgap smaller than the substrate. In our case the GaAlAs layer has the bandgap larger than the GaAs substrate. Therefore this technique can be used only in a destructive mode if the GaAs substrate can be etched away leaving the thin GaAlAs layer for measurements. This approach did not seem to be attractive and therefore we looked into the possibility of deconvolving the reflection data. The reflection measurements would be ideal, however, the experimental measurements did not indicate any structure over the measured spectral range and therefore it does not appear to be sensitive to the grading which we wish to estimate. In section 3.2 we present the theoretical calculations for the optical reflection from a graded GaAlAs layer which confirms this observation. For these reasons, the optical techniques do not appear to be useful for estimating the compositional grading.

Another non-destructive technique for profiling GaAlAs graded composition layer is the Rutherford backscattering analysis. We have successfully used this technique to obtain the composition profile of our LPE grown layers. The details of this technique are not easily accessible in the literature and are therefore described in Section 3.2. The major limitations of this technique arise from (a) the detector resolution and (b) the fact that we are trying to profile a light element (Al) in a heavy background (GaAs). The detector resolution affects the accuracy of the analysis at the two depth boundaries of the impurity element being profiled. Since Al is lighter than GaAs, it causes the backscattering signal from Al to overlap with the GaAs signal and therefore requires a subtractive procedure for analysis. This limits the accuracy of the quantitative evaluation at

low Al concentration values. However, the results obtained on our graded layers and described in section 3.2 demonstrate the usefulness of this technique.

The other quantitative profiling techniques, for which we have the facilities, are the energy dispersive x-ray analysis in the SEM and the sputter-Auger electron analysis. Both of these techniques are destructive in nature. In the sputter-Auger electron analysis, the region under analysis is physically sputtered away while in the SEM analysis the sample has to be cleaved to expose the cross-section of the active region to be analyzed. The spatial resolution of the SEM x-ray analysis is limited by the volume of the material excited by the incident electron beam. At low beam voltages, around 5 KV where reasonable x-ray counts can be obtained, the spatial resolution is limited to about 0.2μm. For analyzing submicron thick GaAlAs layers, this technique is very crude. In addition, the cleaving process is not reliable for obtaining good flat cleaves right up to the surface.

The spatial resolution obtainable from the sputter-Auger electron analysis technique can be very good, around 20Å. However, it requires raster-scanning by the sputtering ion-beam in order to get a flat area in the center of the scanned area for Auger-electron analysis. We have utilized such a facility available at Stanford University and the results are presented in section 3.2.

2.2.3. Device Optimization

The performance optimization of a new device structure like the graded bandgap solar cell for this program, is a feedback process involving a continuous evaluation of the experimental results. For this program we started out with a n on p device structure based on the theoretical optimization studies done by Dr. James A. Hutchby of NASA, Langley.[3] The experimental results are presented in Section 3. From our composition profile measurements we found that the thickness of the graded region in the $Ga_{1-x}Al_xAs$ layer did not exceed 0.5μm. The calculated optimum graded layer thickness for n/p structure is 1μm.[3] In addition, the measured

efficiency values were lower than the calculated values because of smaller open circuit voltage and fill factor. For comparison and evaluation purposes, we started working on the p on n structures. These studies led to the conclusion that p on n structure is superior for obtaining good fill factor and open circuit values. Since Zn was used as the p-dopant in the GaAlAs layer, it resulted in Zn-diffusion into the n-GaAs substrate during the LPE growth process. The resulting solar cell structure is then a graded bandgap heteroface solar cell illustrated in Fig. 1. As reported in section 3.4, it results in better I-V characteristics expected from the p-n homojunction in GaAs, which in turn yields improved open circuit voltage and fill factor. We feel that this is the optimum device structure with the constraint imposed by the LPE growth process on the graded region thickness (<0.5μm). Later optimization studies by Hutchby[18] on p on n structures indicate that the optimum graded region thickness for p-GaAlAs is 3.5μm. At this time, it is recommended that MBE growth technique be developed to fabricate such structures.

3.0 RESULTS

3.1 GROWTH OF THE GRADED BANDGAP SOLAR CELL BY THE LPE MELT MIXING TECHNIQUE

As discussed in section 2.2.1, our objective was to grow a graded bandgap solar cell utilizing an GaAlAs layer graded in composition from zero AlAs to ~35% AlAs over a distance of at least 0.5μm. In order for the cell to have good spectral response at short wavelengths, it is crucial that the layer be graded all the way to the surface. Otherwise the high surface recombination velocity dominates any electric field that may be present near the surface, resulting in poor short wavelength response.

Our initial efforts were directed at growing n/p solar cells with the structure shown in Fig. 2. The LPE growth of the Ge-doped GaAs base layer (p-type) results in a high quality layer with long diffusion length which assures excellent spectral response at long wavelengths. Next, the growth of a 0.5μm Sn-doped GaAs layer (n-type) provides a good p-n homojunction and reduces the series resistance of the cell. And finally, the growth of a Te-doped graded bandgap GaAlAs layer (n-type) results in a built-in electric field that accelerates photogenerated holes away from the surface where the recombination velocity is high. This results in good short wavelength spectral response.

Fig. 3 shows the schematic of the double-slider boat used for the growth of the structure in Fig. 2. Slider 1 carries the three melts required for the growth of the three layers. Slider 2 has two windows through which the melts can be brought into contact with the substrate. For growing the solar cell structure, both the sliders are first aligned as shown. When conditions are ready for growth to begin, Melt 1 is brought over the substrate to grow the p-GaAs base layer. In doing so both sliders are moved together. Next, both sliders are again moved together so that Melt 2 is stopped and then Slider 1 is moved further to bring Melt 3 over the substrate. During this time a portion of Melt 2 is confined over the substrate resulting in the thin n-GaAs layer growth. Then as Melt 3 mixes with

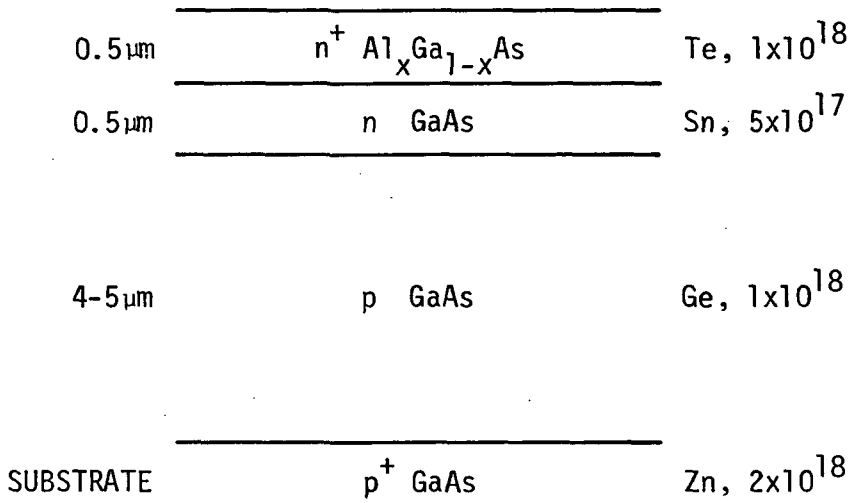

Fig. 2 Structure of the n/p graded bandgap solar cell. The $Al_xGa_{1-x}As$ layer is graded from x = 0 at the interface to x = 0.35 at the surface.

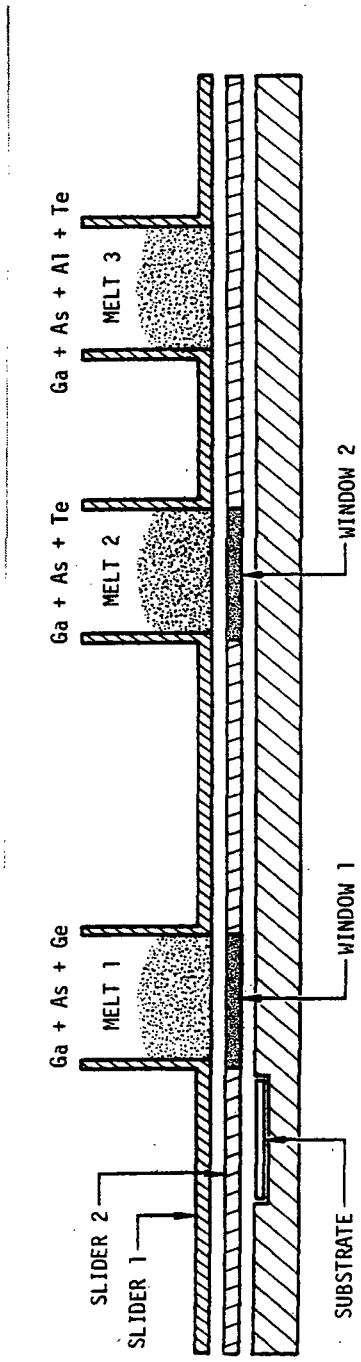

Fig. 3 Schematic representation of the double-slider boat arrangement for the LPE growth of the graded bandgap GaAlAs/GaAs solar cell.

the confined melt, the n-layer composition changes from GaAs to GaAlAs as the growth continues. The grading profile is expected to depend on a combination of the growth rate and the details of the mixing process.

The LPE growths take place in an ultra-pure hydrogen atmosphere at 1 atmospheric pressure. All boats are machined from high purity graphite. The boat is supported in the quartz growth tube by a quartz boat holder. This boat holder has a cooling cavity with a flat upper surface directly under the substrate. Growth is initiated by blowing room temperature nitrogen gas into the cooling cavity, which cools the substrate relative to the melt. A typical cooling rate is 3-4°C/min. The growth time for a 4-5μm thick GaAs layer is typically 1.5 min. All growths were made at ∿750°C. A typical melt weight is 4-5 gm for growth on a 0.5 x 0.75 in. substrate. Melts are equilibrated at the growth temperature for 30-45 min prior to growth. All growths were made on (100) GaAs substrates. The above are general conditions for most of the growths made under this contract; any changes will be noted as the following different melt-mixing techniques are described.

Following the removal of the epitaxial growth from the furnace, one of the first evaluation procedures performed is to measure the spectral response. A small piece ∿2.5 mm square is cleaved from the growth. This piece is mounted in a holder to make electrical contact to the front and back surfaces. Since the contacts are non-ohmic reverse bias is applied across the p-n junction of the test piece so that the photocurrent can be measured. Most of our spectral response curves are measured on such test pieces and are representative of the response measured on the fabricated cells with ohmic contacts. The spectral response is measured using a modified dual beam Cary 14 spectrophotometer. Monochromatic light is incident on the test piece through a 1 mm diameter hole. Our photoresponse measurement system includes a PbS detector in the reference beam that provides feedback to partially correct the light incident on the test piece for constant number of photons as a function of wavelength. Final correction of the measured spectral response curve, corrected for constant number of photons, is made using a calibrated UV-enhanced Si photodiode, calibrated by the

manufacturer.

Cells are fabricated by evaporating front and back ohmic contacts, mesa etching and cleaving to produce individual cells, and finally packaging and wire bonding. For p-type GaAs or GaAlAs we used evaporated Ag-Mn (4% Mn); for n-type material Au-Ge (12% Ge). After evaporation the contacts are sintered at 450°C for 4 min in hydrogen atmosphere. Mesa etching is done using standard photolithography techniques.

All the cells we made using this double-slider boat had poor spectral response at short wavelengths, but we found that the response could be significantly improved by carefully etch-thinning the GaAlAs layer. Fig.4 shows the spectral responses of a cell before and after etch-thinning (not anti-reflection coated). The spectral response for the as-grown surface shows a relatively sharp decrease in response around 0.65μm which then decreases linearly to zero around 0.38μm. This decrease at ~0.65μm is due to an ungraded region near the surface. After etching to remove this region, the response increases in the short wavelength regions. This improvement indicates that the built-in field in the graded region does help the collection at short wavelengths. Using the proton backscattering technique to analyze the grading, we found that the graded portion is ~1000 - 2000Å thick followed by an ungraded portion to the surface of roughly the same thickness. This will be described in detail later.

Although we were successful in obtaining good short wavelength response using the etch-thinning technique, it was found to be impractical even for small area cells (65 mil x 65 mil). The reason is that the etching was very non-uniform causing the surface to become rougher.

Our growth efforts were then directed to the problem of eliminating the ungraded region next to the surface. The obvious way of doing this is to slow down the growth rate so that the growth can be terminated (by wiping Melt 3 off the substrate) before the ungraded portion begins to grow. We were not successful in doing this however. No matter how fast the sliders were moved, and in spite of all efforts to slow the growth rate by reducing the

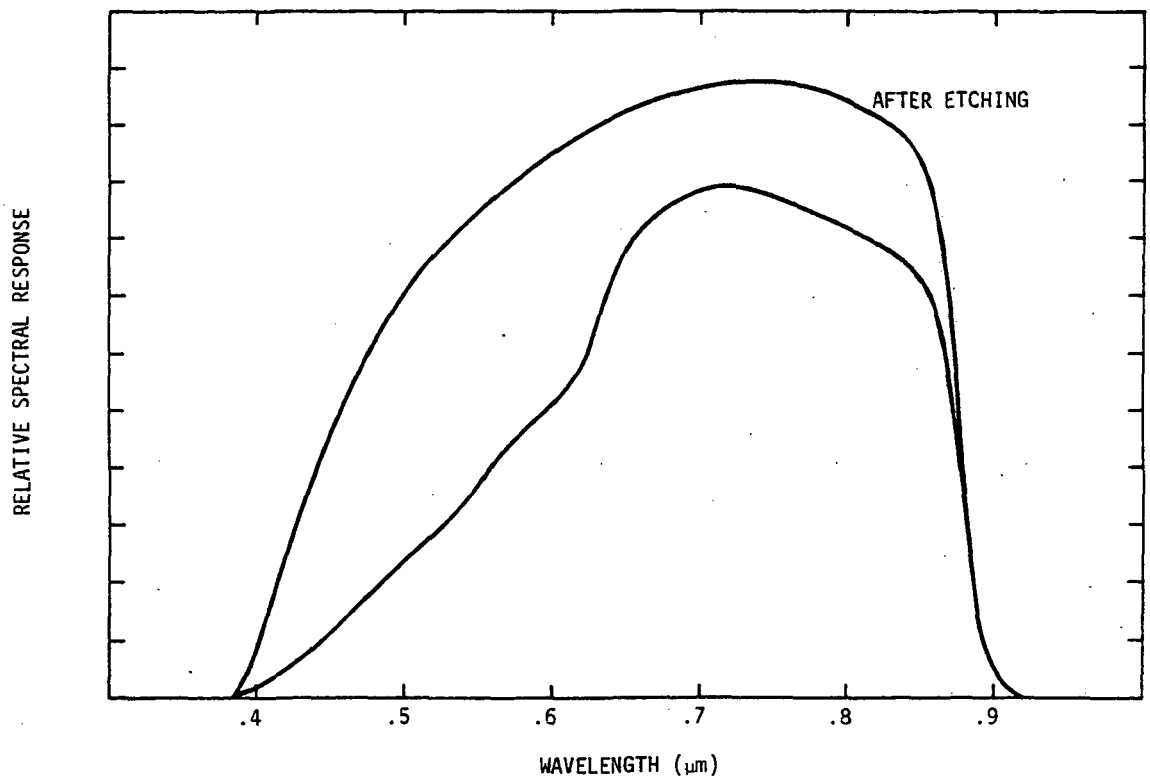

Fig. 4 Spectral response of an n/p graded bandgap solar cell without AR-coating. The curve obtained before the cell was slightly etched shows a response drop of ∿0.65μm representing a thin ungraded region near the surface.

degree of supersaturation, an ungraded portion always began to grow before the growth could be terminated. The best we could do was to minimize this ungraded length.

Fig. 5 shows the spectral response of an anti-reflection coated cell grown such that the ungraded GaAlAs portion near the surface is minimized. Consequently this cell was not etched to remove the ungraded portion. The active area plus contact area for this cell is 65 mil x 65 mil. The computed J_{sc} is 26.8 ma/cm^2. A 27.7ma/cm^2 J_{sc} value was measured under simulated AMO conditions using a Spectrolab Solar Simulator at the Rockwell Space Division. Measured V_{oc} = 0.88 V and fill factor of 0.76 lead to an AMO efficiency of 13.6%. The short circuit current could be much larger if the short wavelength spectral response were significantly improved.

The short wavelength response would be better if the grading length was increased from the observed 1000 - 2000Å. The grading length can be increased by slowing down the mixing process, but this proved difficult to do with the given boat geometry. The mixing of two melts in this boat at a growth temperature of 750°C appeared virtually instantaneous, as viewed through the transparent furnace.

Fig. 6 shows two of the best spectral response curves obtained for non-AR coated cells that were etch-thinned. The calculated J_{sc} for both these cells is about 22 ma/cm^2 which could be increased to more than 28 ma/cm^2 with anti-reflection coating. Again, these are small area cells (65 x 65 mil).

The main problem with the double-slider boat is that the mixing of the confined portion of Melt 2 with Melt 3 is too rapid. The confined portion of M2 weighed about 2 gm, while the weight of M3 was typically 0.6-1.0 gm. Larger weights of M3 resulted in faster mixing. The too-rapid mixing produces a short grading length followed by an ungraded region extending to the surface. While this grading length of 1000 - 2000Å is shorter than the desired 5000Å or longer, it is still much longer than the ~100Å grading length we have observed for "abrupt" heterojunction growth of

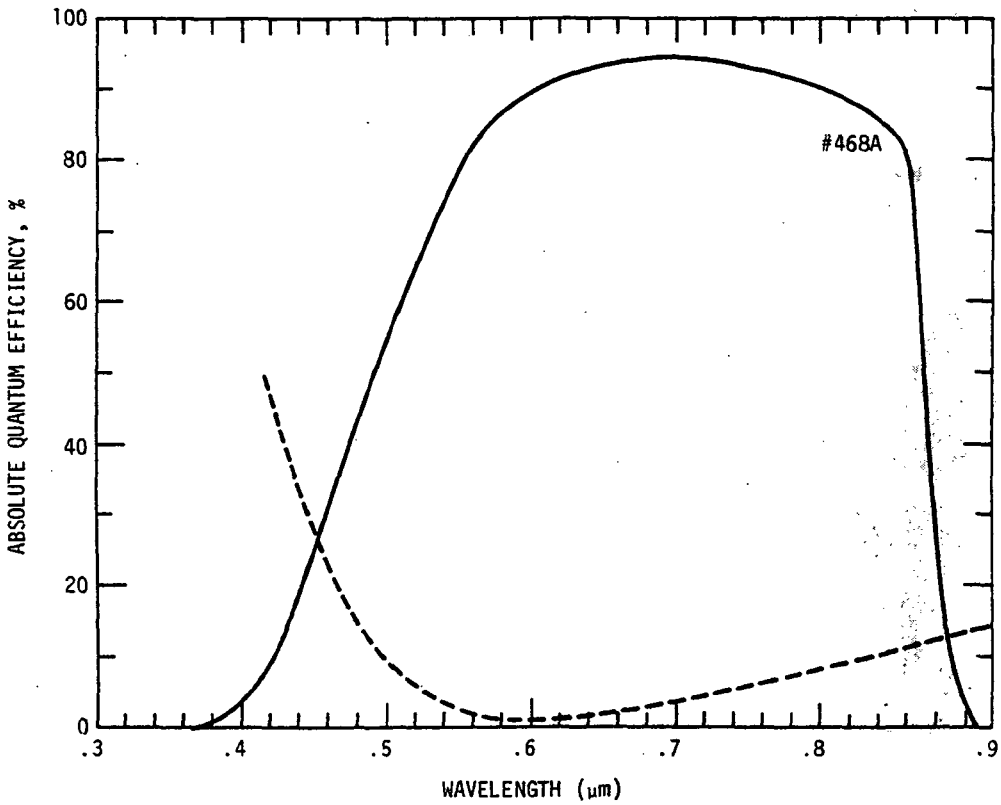

Fig. 5 Spectral response of an AR-coated n/p graded bandgap solar cell. The computed AM0 J_{sc} for this cell is 26.8 mA/cm^2 while the measured J_{sc} under simulated AM0 conditions was 27.7 mA/cm^2. The measured values of V_{oc} = 0.88V and a fill factor of 0.76 lead to an AM0 efficiency of 13.6%. The dashed curve shows the percent reflection loss from an AR-coated GaAs control sample with the same AR-coating that is on the cell.

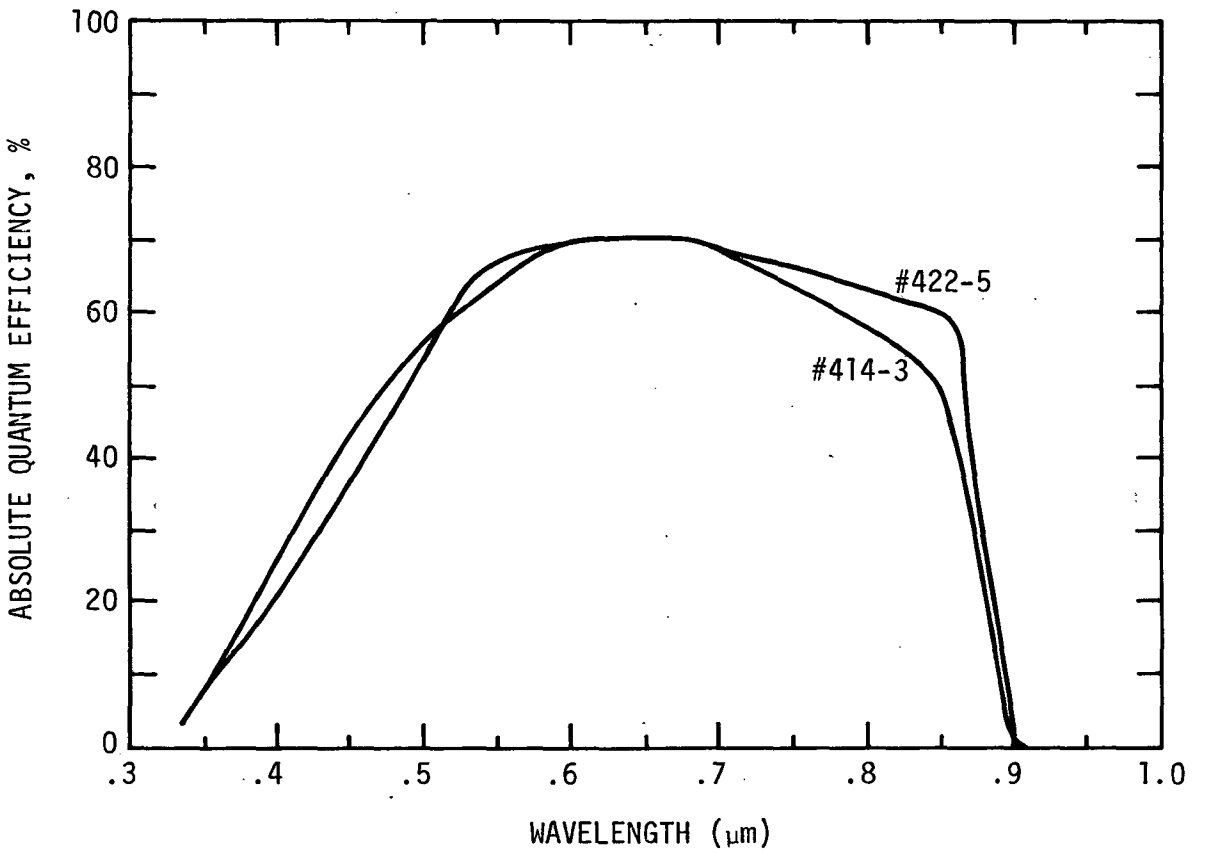

Fig. 6 Spectral responses of two n/p graded bandgap solar cells without AR-coating grown in the double-slider boat. The calculated AMO J_{sc} for both cells is 22 mA/cm^2. Both cells were slightly etched to improve the short wavelength response.

$Al_{.85}Ga_{.15}As$, as measured by sputter etching/Auger profiling.

Therefore, our next phase of work was directed toward using a new boat geometry utilizing slower melt mixing to increase the grading length. Fig. 7 shows a schematic of the way melt mixing was done. A GaAs epitaxial layer is grown on the substrate from a melt having the geometry shown. Then a (Ga + Al + dopant) melt is dropped on to the first melt during growth. The degree of mechanical mixing of the two melts, as well as the diffusion of Al to the substrate are controlled by varying the height of GaAs melt in the chimney. This in turn should control the grading profile.

For these growths we made p/n cells to compare with our previous experience with n/p cells. Two alternative structures for p/n cells are shown schematically in Fig. 8. In (a), the structure is almost the exact complement of the structure for n/p cells shown in Fig. 2. The major difference is that the p-GaAs layer is thicker than the complementary n-GaAs layer in Fig. 2 due to the difference in resistivity between n and p type layers of the same doping level. The use of Zn as the p-type dopant is often desirable, as described in section 3.4. However, the vapor pressure of Zn is so high at these growth temperatures that an n-type GaAs layer cannot be grown. Fig. 8(b) shows the p/n structure when Zn is used as a dopant.

Many growths were made using this boat varying the growth conditions to improve the spectral response. We found that the higher the GaAs melt extended up into the chimney, the less Al was seen in the growth, as measured by x-ray analysis in the SEM. The sepctral response was found to improve with increasing AlAs composition up to ∿40% AlAs, and consequently less GaAs melt in the chimney. A typical spectral response using this technique is shown in Fig. 9. In this growth only a very small portion of the chimney neck was utilized so that more Al would be incorporated into the growth. The growth time after mixing was just 5 sec. and the surfaceecomposition was found to be $Al_{.42}Ga_{.58}As$. The long tail indicates there is some grading, but the poor response below ∿0.66μm indicates an ungraded AlGaAs region exists next to the surface.

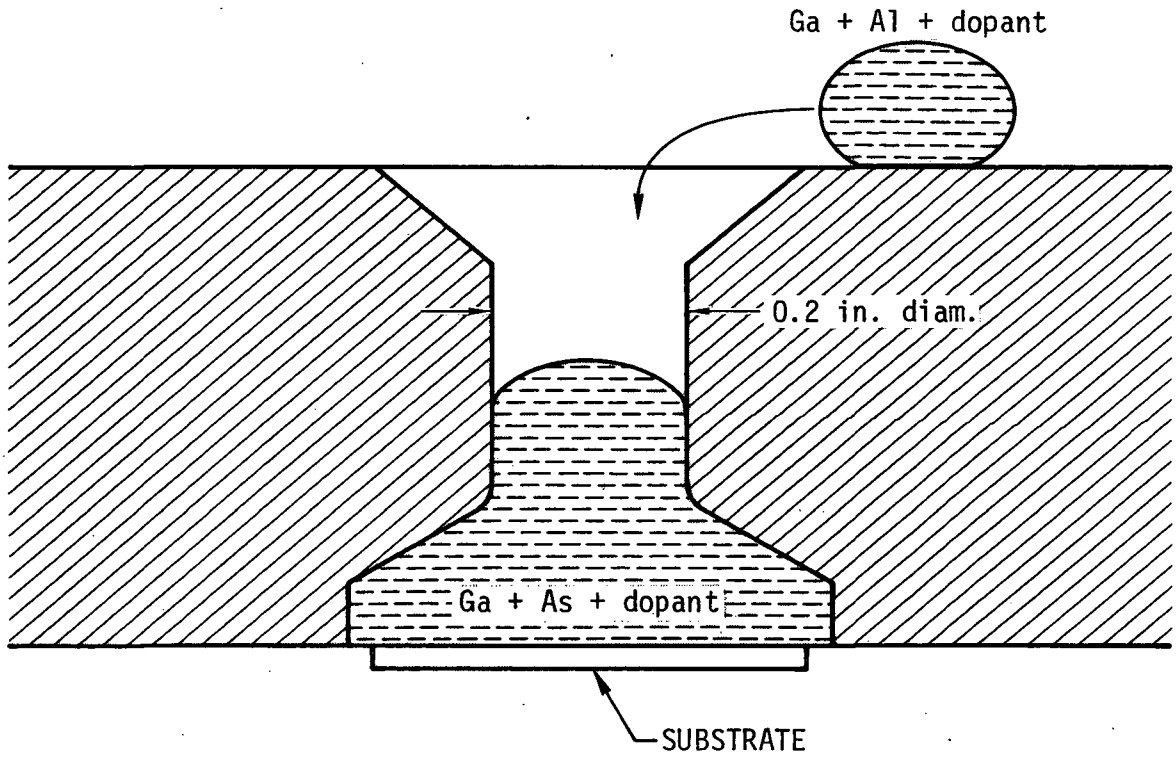

Fig. 7 Schematic of the melt mixing portion of the new LPE chimney boat.

0.5μm	p^+ $Al_xGa_{1-x}As$	Be, $1x10^{18}$
1-2μm	p^+ GaAs	Ge, $1x10^{18}$
4-5μm	n GaAs	Sn, $5x10^{17}$
SUBSTRATE	n^+ GaAs	Si, $2x10^{18}$

(a)

0.5μm	p^+ $Al_xGa_{1-x}As$	Zn, $1x10^{18}$
1-2μm	p^+ GaAs	Zn, $1x10^{18}$
SUBSTRATE	n^+ GaAs	Si, $2x10^{18}$

(b)

Fig. 8 Two structures of the p/n graded bandgap solar cell. The $Al_xGa_{1-x}As$ layer is graded from $x = 0$ at the interface to $x = 0.35$ at the surface.

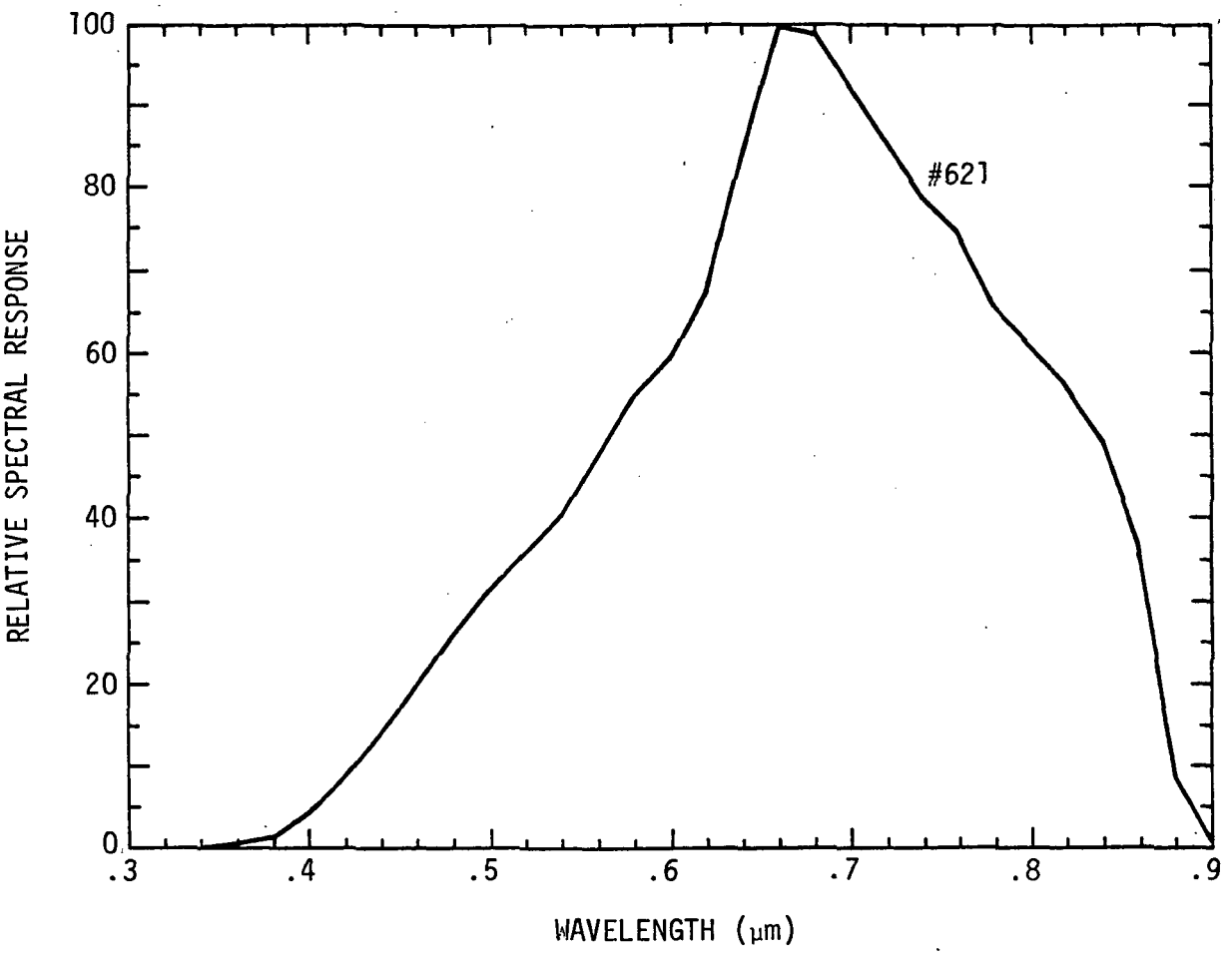

Fig. 9 Spectral response of a p/n graded bandgap solar cell without AR-coating grown in the new chimney boat.

Our results using the chimney boat were disappointing relative to our expectations. The grading profile appeared different, but the low wavelength spectral response was still poor. In addition, results were not reproducible due to slight differences in weight of melts, degree of mixing speed from growth to growth, and growth non-uniformity caused by the mixing mechanics.

While Fig. 9 shows a typical spectral response from growths made in this chimney boat, Fig. 10 shows an untypical response from a growth made in the same boat, corrected for reflection. For comparison, also shown is the response of an ungraded heteroface cell grown in the same boat. The response curve labeled "Graded" was on a sample with ∿0.25μm thick $Al_xGa_{1-x}As$ graded layer with x = .35 at the surface while the curve labeled "Abrupt" was on a sample with ∿0.3μm constant composition $Al_{.35}Ga_{.65}As$. The best results were obtained using an M1 weight of ∿2.2 gm and M2 weight of ∿0.5 gm. This figure shows clearly the significant improvement in spectral response that can result when the GaAlAs layer is graded.

One problem that concerned us up to this time was the resulting degree of As saturation in the melt after mixing. The addition of Al to the melt strongly decreases the As solubility, leading to very fast growth rates and the formation of GaAlAs crust that grows on the melt surface. In these growths the melt was always very supersaturated after mixing. Our next step was to see what would happen if this degree of supersaturation was reduced.

For this experiment we used a different boat. The mixing scheme is shown schematically in Fig. 11. The mass of the (Ga + Al + dopant) melt can be made any reasonable size, unlike the case with the chimney boat, so that the resulting melt after mixing is just barely supersaturated. This would slow down the growth rate and thus change the grading profile.

Fig. 12 shows spectral responses for two different growths using this boat geometry. In growth #758 the melt after mixing was just barely supersaturated with As. Growth continued for ∿2 sec. and the surface

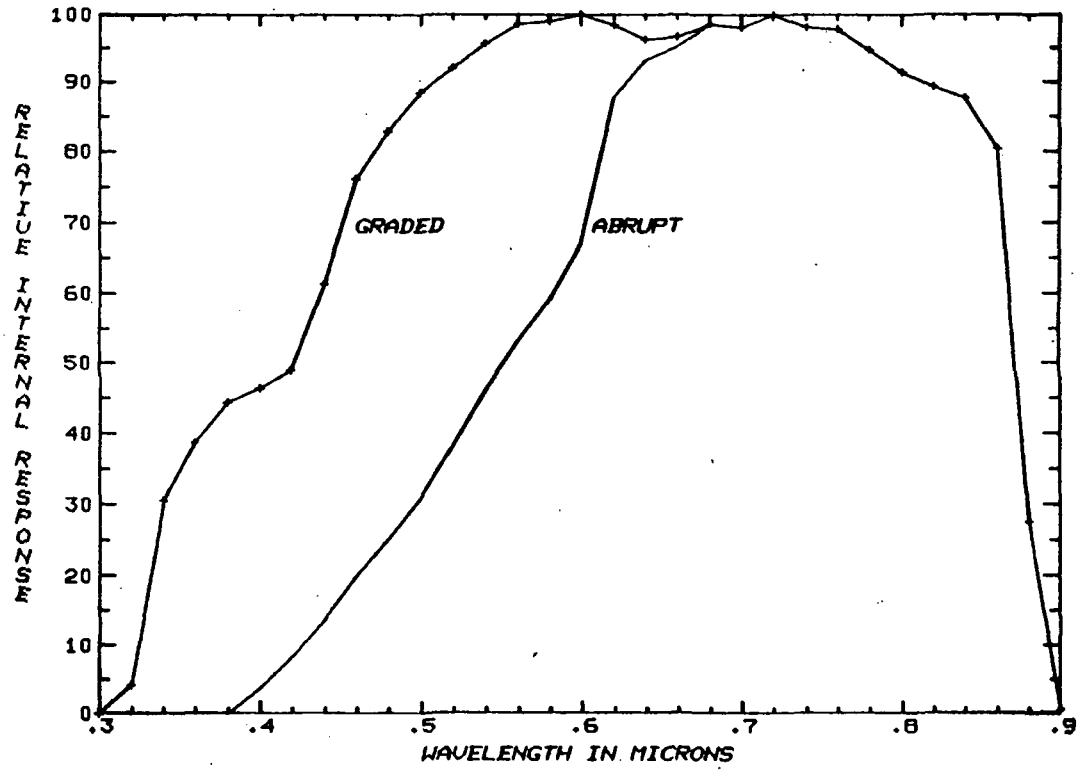

Fig. 10 Measured spectral response of a graded bandgap GaAlAs/GaAs solar cell. For comparison, the response from an ungraded heteroface with similar composition is also shown.

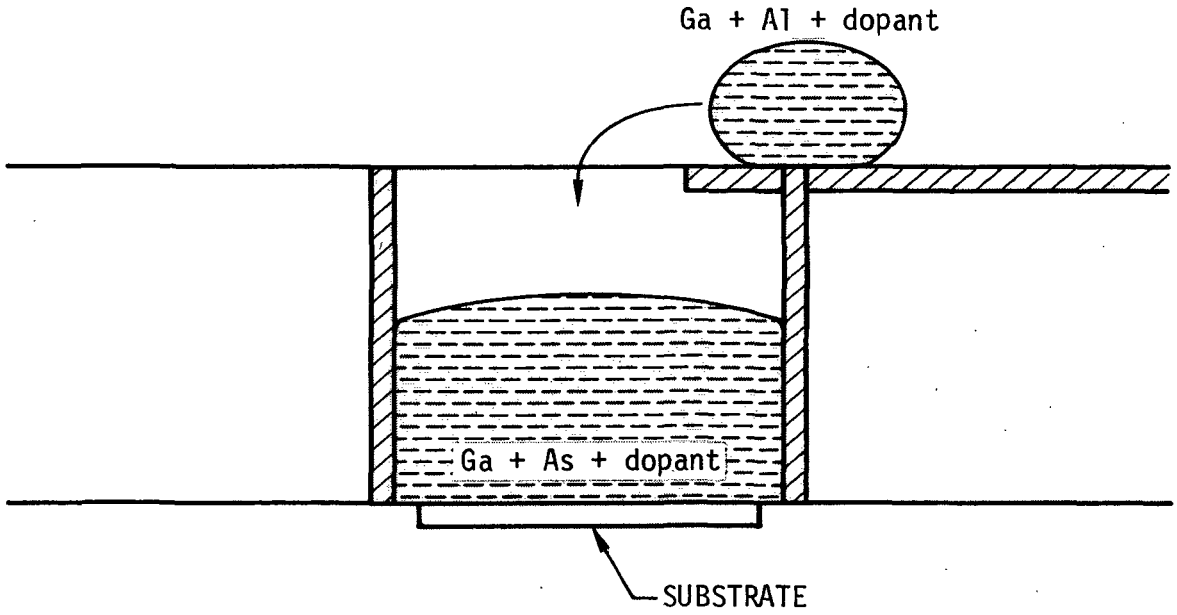

Fig. 11 Schematic of the melt mixing portion of a new boat for the LPE growth of the graded bandgap solar cell.

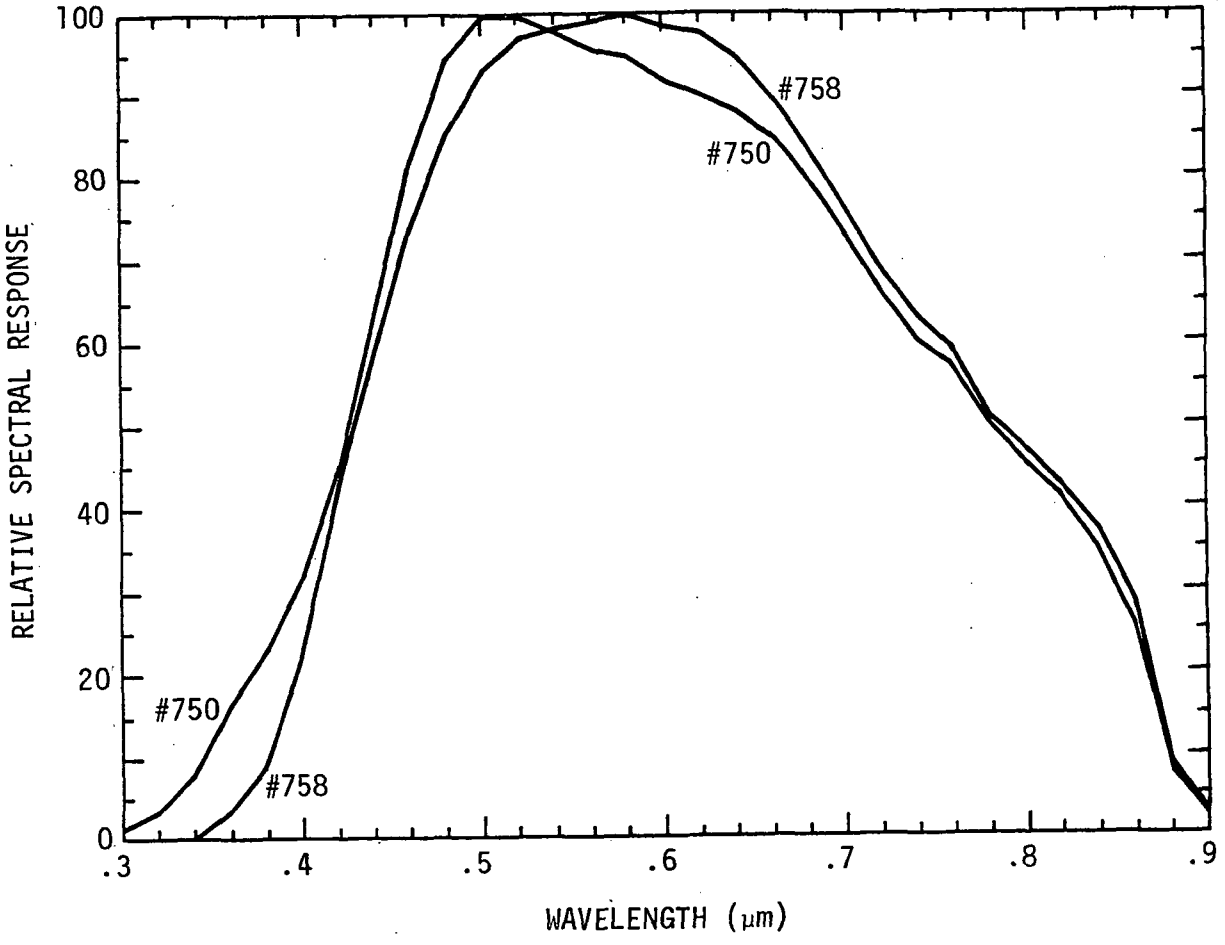

Fig. 12 Spectral responses of two p/n graded bandgap solar cells without AR-coating grown in the boat shown in Fig. 7. The melt mixing for growth #750 resulted in a very supersaturated melt whereas in #758 after melt mixing the melt was only slightly supersaturated.

composition of the resulting growth was $Ga_{.68}Al_{.32}As$. Less AlAs was seen on the surface than in growth #758 because less Al was in the melt. The melt weights for growth 750 were M1 = 3.69 gm, M2 = 0.49 gm; for growth 758: M1 = 2.71 gm, M2 = 1.57 gm. It is reasonable to assume that because of the better short wavelength response, #750 has a better grading profile.

Comparing the spectral responses of growths #750 and #758 with that of growth #621 in Fig. 9, it seems that the geometry of mixing (boat geometry) plays the major role in determining spectral response shape at short wavelengths. The short wavelength response of these growths represents a large improvement over earlier growths. Unfortunately the long wavelength response is less than it should be because the p-GaAs layer is too thin. From our experience with other cells we know that this layer can easily be made thicker to give good long wavelength response without affecting the shape of the response at short wavelengths.

Next we tried multiple-melt mixing. We used the same boat with mixing geometry shown in Fig. 11, except modified so that four (Ga + Al + dopant) melts could be dropped in successively. The idea was to increase the grading length by increasing the melt Al composition in discreet steps rather than in one almost instantaneous step as previously done. Fig. 13 shows spectral response curves for two growths made using this technique. In growth #677 three melts were dropped so that the GaAlAs composition increased to 9% AlAs, then 18%, and finally 27%. The melts were mixed quickly and the growth then quickly terminated. Growth #696 was done in an identical manner, except that a fourth melt rich in Al was dropped in so that the final growth composition was $Al_{.85}Ga_{.15}As$. That is, the GaAlAs composition increased from zero to 5%, then to 18%, 27%, and finally 85% AlAs. In both growths the weight of M1 was $\sim$3.5 gm. The weights of the four mixing melts vaired from 0.37 to 0.54 gm. Individual weights were chosen so that after each mixing the resulting melt on the substrate was just barely supersaturated. This procedure should slow down the growth rate. The spectral response curves are very similar except that #677 shows significantly better response at very short wavelengths. It seems likely that this

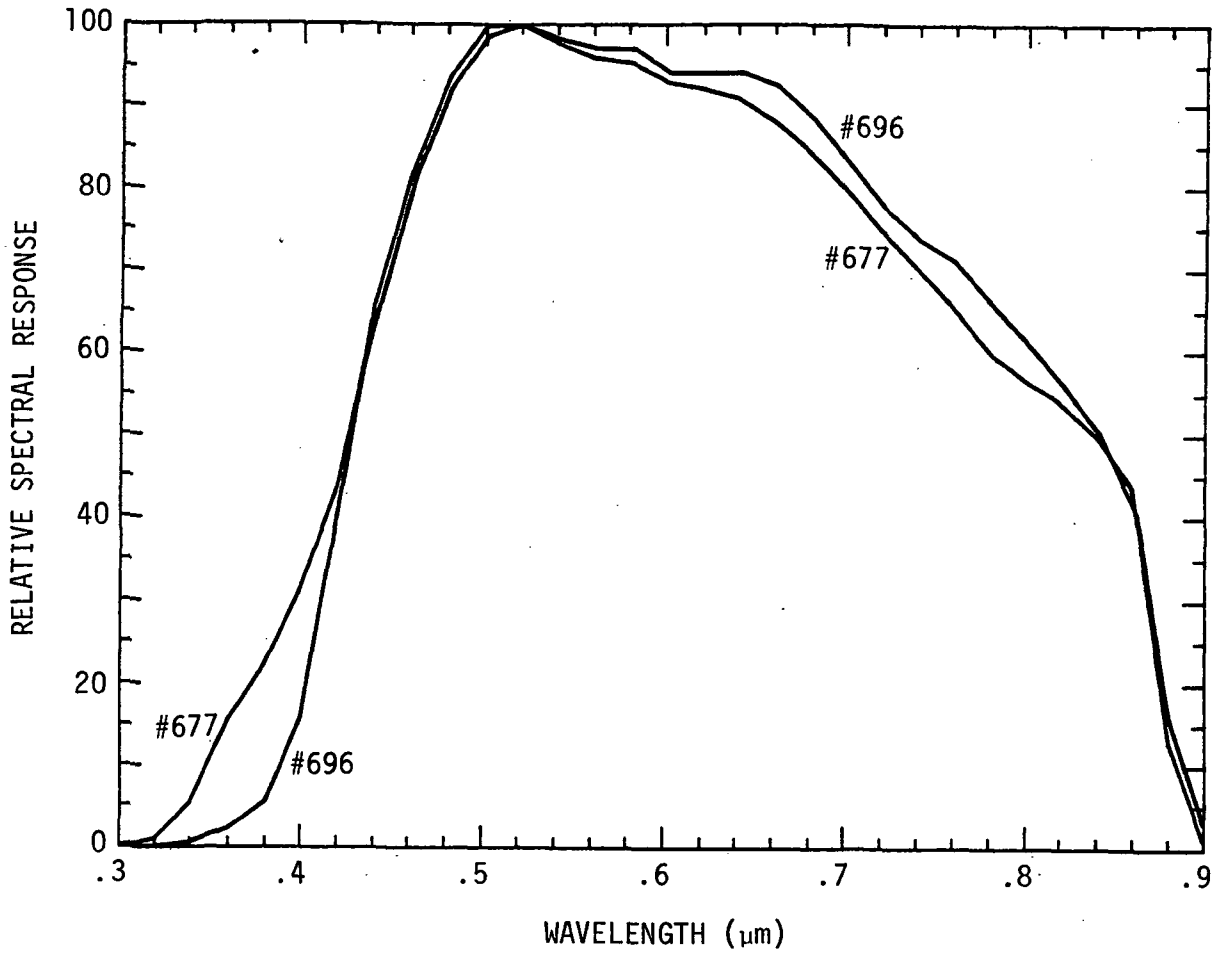

Fig. 13 Spectral responses of two p/n graded bandgap solar cells without AR-coating grown by the multiple melt mixing technique. In growth #677 the surface composition is $Al_{.27}Ga_{.73}As$. Growth #696 was identical to #677 except that an additional melt drop occurred so that the surface composition is $Al_{.85}Ga_{.15}As$.

growth technique suffers from the same problem we have observed all through this program: ungraded GaAlAs grows near the surface before the growth can be terminated. For this reason there is no improvement in short wavelength response compared to all the other graded bandgap growths we have made.

3.2 COMPOSITION PROFILING OF THE $Ga_{1-x}Al_xAs$ LAYER

As mentioned in the approach section 2.2.2, the measurement of the composition profile of the graded GaAlAs layers was attempted by a number of techniques. Our goal was to develop one reliable and non-destructive technique capable of providing the quantitative composition profile. In the following paragraphs, we describe a number of techniques evaluated for the purpose. We found the Rutherford backscattering analysis technique to be suitable for our purpose. This technique was, therefore, developed and the details of the analysis procedure are also described below.

3.2.1 Scanning Electron Microscope Analysis

At the beginning of this program we used SEM-x-ray analysis to estimate the composition profile of the graded GaAlAs layer. As mentioned in section 2.2.2, this technique depends on the quality of the cleave obtained on the sample. Usually the cleavage is not perfect near the surface if there is a thin grown layer. We purposely grew a thick GaAlAs layer by increasing the growth time to avoid any artifact in the SEM measurement. Fig. 14 shows the aluminum concentration profile in one of the early graded bandgap solar cell structures. It shows that the Al-concentration increases from zero to 50 atomic percent in about 0.5μm distance from the interface. Then the Al-concentration keeps on increasing slowly to about 70 atomic percent at the surface. For the actual solar cell growth, we tried to stop the growth earlier so that the grading would extend all the way up to the surface. This measurement technique is however limited in resolution to about 0.2μm when used with 5 KeV electron beam. At lower beam voltages required for higher resolution, the x-ray count rate falls below acceptable levels. Since the graded region in the growths was only about one half of a micron, we started investigating other profiling techniques.

3.2.2 Optical Techniques

We considered using the optical measurement analysis techniques for profiling the GaAlAs layers. We had previously developed a profiling technique[17] using the optical transmission through thin films. However,

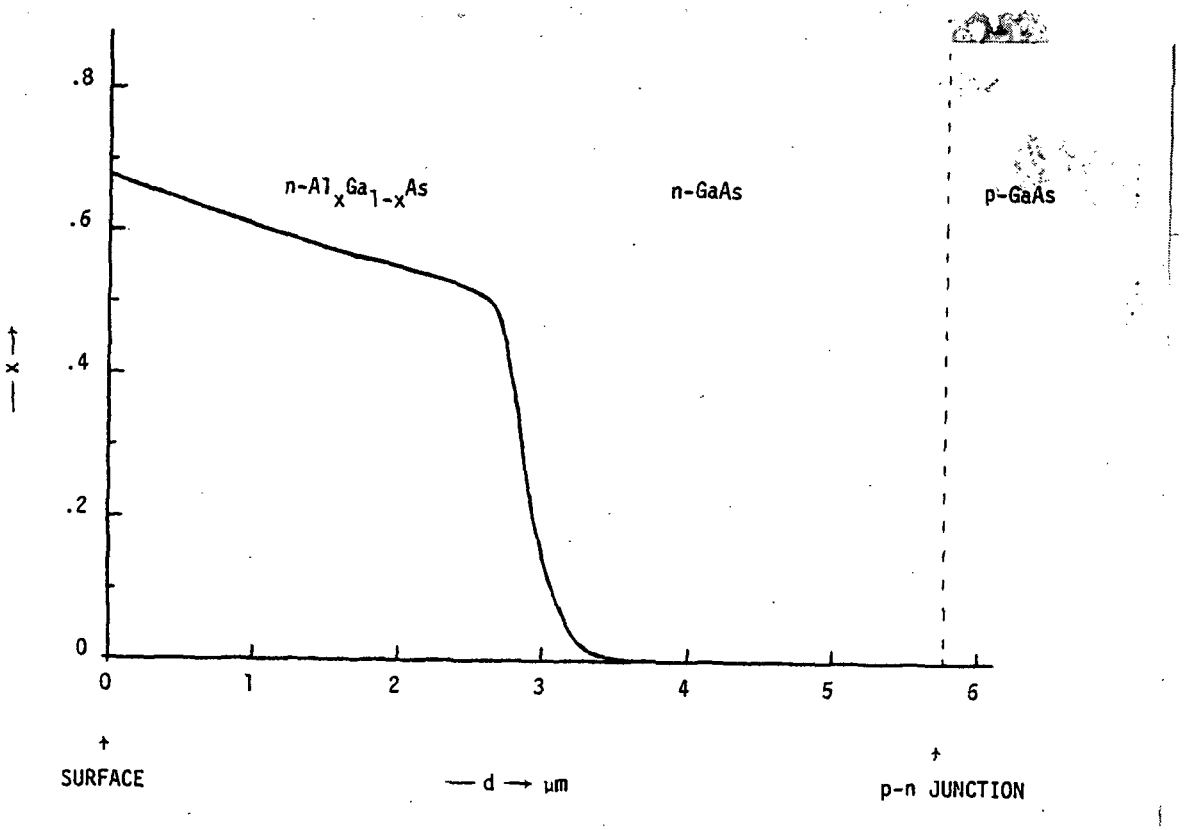

Fig. 14 The aluminum concentration profile of a graded bandgap layer as obtained by the x-ray measurements on SEM.

as mentioned in the approach section, this technique is convenient to use for thin films only if the substrate material is optically transparent in the wavelength range when the thin film is optically absorptive. In our case this technique can be used only in a destructive mode if the GaAs substrate can be etched away leaving the thin GaAlAs layer for measurements. We tried some selective etching techniques, but gave up because this procedure is very time consuming and the resulting thin membrane of GaAlAs layer is too fragile to handle.

Next, we looked into the possibility of deconvolving the reflection data. Fig. 15 shows the calcualted reflection coefficient for a number of cases. Curve (a) is for the bare GaAs, curve (b) is for the linearly graded surface layer changing from GaAs to GaAlAs with 1.9 eV bandgap at the surface. Curves (c_1) and (c_2) are for an ungraded GaAlAs layer with 1.9 eV bandgap and 0.25 and 0.75μm thickness respectively. For the graded case (curve (b)), the reflection did not change if the layer thickness and therefore the bandgap gradient is changed. The experimental measurements on various graded and ungraded GaAlAs layers confirmed these calculated results. Since the reflectivity from these graded GaAlAs layers is not sensitive to the composition profile we wish to estimate, we abandoned these optical measurements in favor of other promising techniques.

3.2.3 Rutherford Backscattering Analysis

The principles of application of backscattering to the analysis of surface layers have been described in a review article by Chu et al.[19] When an energetic proton beam is incident on a sample most of the protons penetrate into the material where they lose some energy to the electrons and have a finite chance of having a head-on collision with a lattice atom. At this point they go through an elastic scattering process and some of them suffer a large angle deflection and are back-scattered. The energy spectrum of the backscattered protons contains the depth information in terms of the energy loss. In order to eliminate the channeling effects, the samples were oriented off a major crystallographic axis and then rotated with respect to the incident beam.

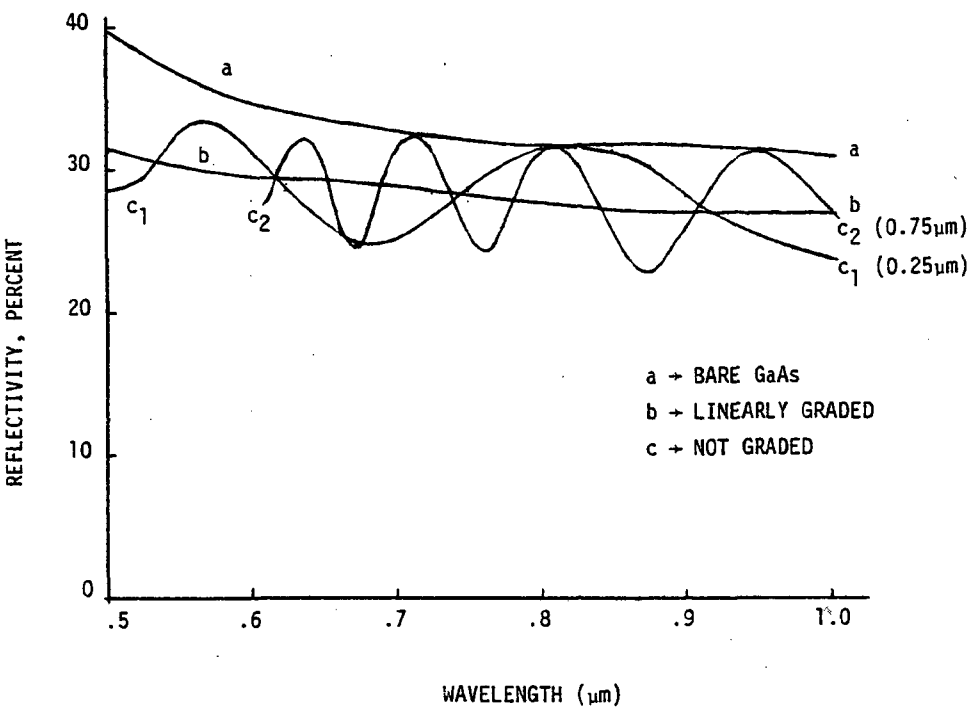

Fig. 15 Computed reflectivity for the GaAlAs/GaAs structures. The curve (a) is for bare GaAs shown for reference. The curve (b) is for a linearly graded GaAlAs layer on GaAs with the bandgap at the surface as 1.9 eV. The curves c_1 and c_2 are for the ungraded GaAlAs layer (E_g = 1.9 eV)[2] on GaAs with layer thickness 0.25μm and 0.75μm, respectively.

For analyzing thin layers of AlGaAs on GaAs, a 400 keV proton beam was utilized. The values of the stopping cross-section (ϵ) of Ga, As and Al for H^+ ions (protons) in the 200-450 keV range of interest are not available in the literature. We have experimentally observed that the back-scattering yield from GaAs and Ge are identical in this energy range, so we can substitute the stopping cross-section of Ge for that of GaAs. The ratio of the stopping cross-section of Ge and Al was experimentally determined.

Fig. 16 shows the backscattering spectrum from a sample of evaporated layers of Ge and Al on a Sapphire substrate for 250 KeV and 450 KeV proton beams. The inset shows the schematic of the scattering geometry. Measurements were made in the 200-450 KeV energy range. From these measurements on Ge/Al samples, we are able to obtain the energy dependence of the Ge stopping cross-section and the ratio of the stopping cross-sections of Al and Ge for protons.

Using the standard notations, the ratio of the heights for the Ge and Al yield, corresponding to the interface position, is given by:

$$\frac{H_{Ge}}{H_{Al}} = \frac{\sigma_{Ge}}{\sigma_{Al}} \times \frac{[\epsilon]_{Ge}}{[\epsilon]_{Al}} \times \frac{\delta(K_{Ge}E)}{\delta(K_{Al}E)} \qquad (1)$$

H_{Ge} and H_{Al} are measured by extrapolating the Ge and Al yields to E_{S1} and E_{S2} respectively. σ is the average Rutherford scattering cross-section and δ is the width of the energy window inside the target at the interface which contributes to the counts outside the target in one channel width of the multichannel analyser.

The last term in Eq. (1) is very near unity and the first term, which is the ratio of theRutherford scattering cross-section, is determined by the geometry of the experimental setup and the atomic number and mass values of the interacting particles. For our setup σ_{Ge}/σ_{Al} ratio is 6.07 and the relative values of σ for Al, Ga and As are 194, 1104 and 1251 respectively. Therefore, we can estimate the middle term which is the ratio of the stopping cross-section of Ge and Al. From our data in the 200 - 450

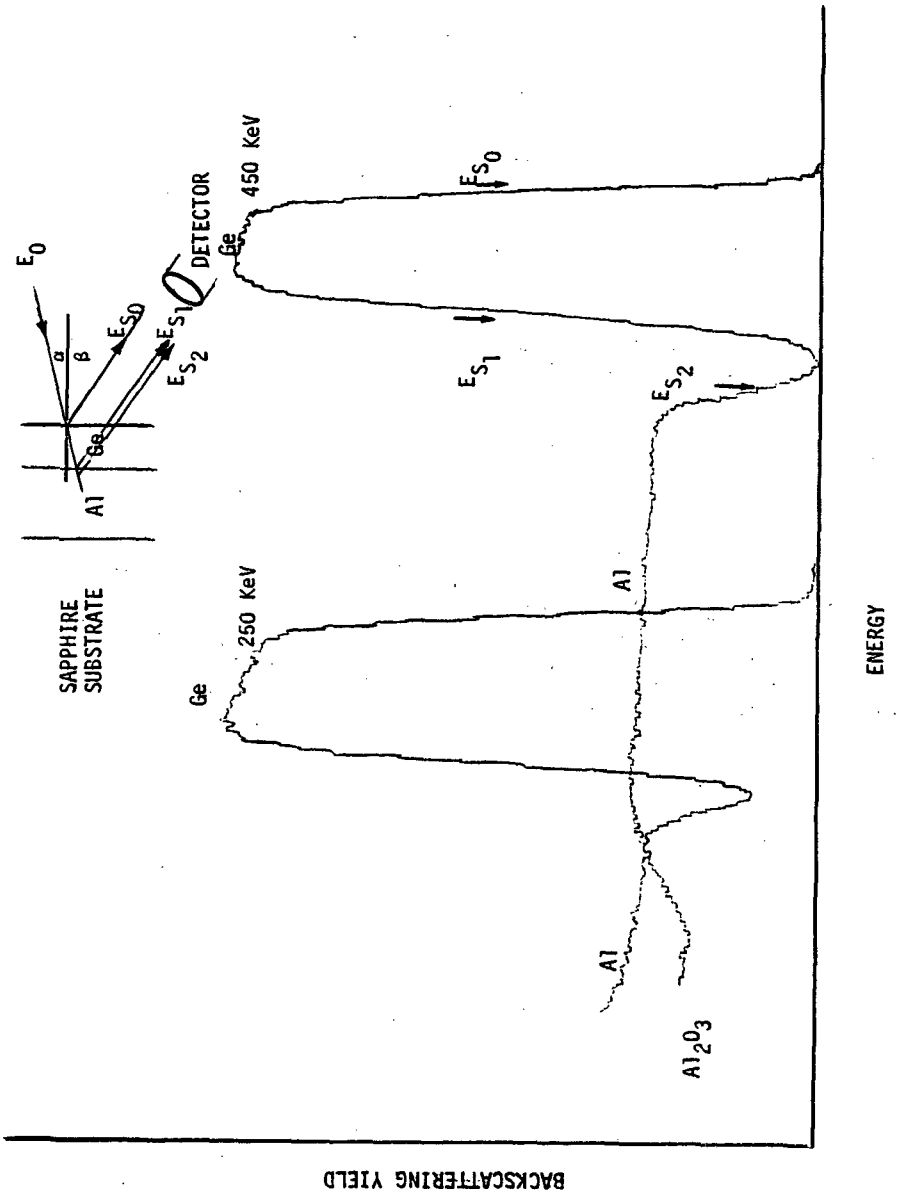

Fig. 16 The backscattering spectra from a sample of evaporated layers of Ge and Al on a sapphire substrate for two different proton beam energies. The inset on the top shows the schematic of the scattering geometry. The experimental setup had $\alpha = 10°$, $\beta = 40°$ and $E_0 = 200$ to 450 KeV.

KeV proton energy range we found this ratio to be independent of energy and has a value of 0.6.

The energy dependence of the Ge stopping cross-section is determined from the width of the Ge yield at different beam energies. The values of E_{so} and E_{s1} are noted for the different incident beam energies. Their difference, $\Delta E = E_{so} - E_{s1}$, is related to the Ge stopping cross-section. In general, in a given range of E, the ε varies according to the relation

$$\varepsilon = \varepsilon_o E^n \tag{2}$$

The value of n is usually small and if ΔE is small compared to E_o, it is reasonable to assume a constant stopping cross-section at an intermediate energy E_x as given by:

$$E_x = \frac{E_{so} \frac{\cos\beta}{\cos\alpha} + E_{s1}}{1 + K_{Ge} \frac{\cos\beta}{\cos\alpha}} \tag{3}$$

The angles α and β are as defined in Fig. 16 inset. Using the relationship given by (3), we can calculate the E_x value for each set of E_{so} and E_{s1} measured between 200 and 450 KeV. Since $\Delta E = E_{so} - E_{s1}$ is proportional to ε, when we plot ΔE vs. E_x on a log plot, we can evaluate the n-value. From our data we were able to obtain a very good linear fit to the log-log plot with a slope of n = -0.295. Thus giving

$$\varepsilon_{Ge} = \varepsilon_o E^{-0.295} \tag{4}$$

for proton energy E in the 200 to 450 KeV range. The absolute value of the stopping cross-section at 400 KeV was obtained from the tables of Northcliffe and Schilling.[20]

This information about the energy dependence of the stopping cross-section and the ratio of Ge and Al stopping cross-sections allow us to carry out the analysis on the graded GaAlAs layers. Figure 17 shows the geometrical details of the measurement set-up and the terminology used for analyzing the backscattering spectra. For clarity, Fig. 17(b) shows the

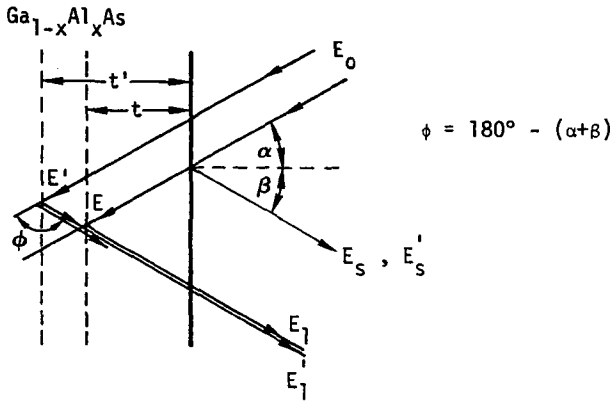

(a)

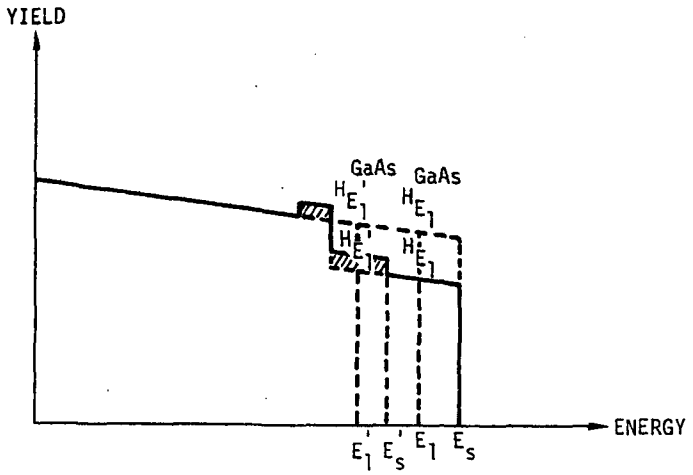

(b)

$$R(E_1) = \frac{H_{E_1}}{H_{E_1}{}_{GaAs}}$$

$$R(E_1') = \frac{H_{E_1}'}{H_{E_1}'{}_{GaAs}} - \Delta R(E_1')$$

Fig. 17 Schematic representation of the backscattering experiment setup (a) and the spectra (b).

idealized spectra for a constant composition AlGaAs layer. The highest energy backscattered protons come from the surface of the sample and their energy E_s is given by

$$E_s = K_{GaAs}\, E_o \simeq K_{Ge}\, E_o \tag{5}$$

where E_o is the incident proton beam energy and K is the kinematic factor which is related to the masses of the incident particle (m) and the stationary particle (M) causing the backscattering. K is given by:

$$K_M = \left(\frac{m \cos\phi + \sqrt{M^2 - m^2 \sin^2\phi}}{m + M} \right)^2 \tag{6}$$

where ϕ is the scattering angle, related to the incident angle α and the reflected angle β by the relation shown in Fig. 17(a). The kinematic factor for the light Al atoms is smaller and therefore the scattering from the Al atoms at the surface shows up at the Energy E_s' $(=K_{Al}E_o)$. This is termed the aluminum edge. The cross-hatched portion in Fig. 17(b) is the backscattering yield due to the Al atoms in the layer. The dotted curve is the backscattering yield expected from a pure GaAs sample and can be seen to be "in-line" with the background spectra coming from the GaAs substrate. The analysis strategy developed by Gamo et al.[21] is to subtract the Al contribution from the total yield spectrum and then compare it with the pure GaAs spectrum to obtain the x-value.

The GaAs spectrum is first established by linear extrapolation of the background spectrum. We assume that the stopping cross-section of AlGaAs is the simple addition of the separate stopping cross-sections for protons in GaAs and in Al, weighed according to concentration (Bragg's Rule). At a detected energy E_1 corresponding to a depth t under the surface, the relative height of the (Ga + As) portion of the backscattering yield as compared to the pure GaAs sample is related to the composition at $t(x_t)$ by:[21]

$$R(E_1) = H_{E_1}/H_{E_1}^{GaAs} = \frac{\sigma_{Ga}(1-x_t) + \sigma_{As}}{(\sigma_{Ga}+\sigma_{As})[1 - \frac{x_t}{2}(1-r)]} \tag{7}$$

where σ is the average Rutherford scattering cross-section and

$$r \equiv \frac{\varepsilon_{GaAs}^{Al}}{\varepsilon} \equiv \frac{\varepsilon_{Ge}^{Al}}{\varepsilon} = 0.6 \text{ (experimental)} \tag{8}$$

and

$$\varepsilon = \varepsilon_o E^n = \varepsilon_o E^{-0.295} \text{ (experimental)} \tag{9}$$

Using the relation (7) and the measured and extrapolated yield heights, one can obtain the composition parameter x_t at the depth t corresponding to the detected energy E_1. From this known composition, one can then calculate the relative height ΔR and the energy E_1' of the Al-signal from this depth t. These values are given by:

$$E_1' = \left[E_s'^{1-n} - (E_s^{1-n} - E_1^{1-n}) \frac{K_{Al}^{1-n} + \theta}{K_{Ge}^{1-n} + \theta}\right]^{1/1-n} \tag{10}$$

where $\theta = \cos\alpha/\cos\beta$ and

$$\Delta R(E_1') = \frac{x_t \sigma_{Al}(E)}{\sigma_{Ga}(E') + \sigma_{As}(E')} \cdot \frac{K_{Ge} + \theta}{K_{Al} + \theta} \cdot \frac{1}{1 - \frac{x_t}{2}(1-r)} \tag{11}$$

where

$$E = \left[\frac{E_1'^{1-n} + \theta E_o^{1-n}}{K_{Al}^{1-n} + \theta}\right]^{1/1-n} \quad \text{and} \quad E' = \left[\frac{E_1'^{1-n} + \theta E_o^{1-n}}{K_{Ge}^{1-n} + \theta}\right]^{1/1-n} \tag{12}$$

The average Rutherford scattering cross-section, σ, varies as E^{-2} and is determined by the geometry of the measurement setup and the atomic numbers and mass values of the interacting particles.

$\Delta R(E_1')$ is the Al contribution to the backscattering yield at E_1'. Therefore, we can now iteratively proceed with the subtraction process as indicated in Fig. 17(b) to obtain the relative height of the (Ga + As) portion of the backscattering yield at E_1' as:

$$R(E_1') = \frac{H_{E_1'}}{H_{GaAs}^{E_1'}} - \Delta R(E_1') \qquad (13)$$

From this value of $R(E_1')$ and the relation (7), we can now obtain x_t, and carry on this iterative process until we reach the substrate with $x = 0$. This analysis technique can be programmed to obtain the continuous profile by initiating the iterative procedure with every channel between E_s and E_s'. The absolute depth scale for the composition profile thus obtained was calculated using the relationship derived by Behrisch and Scherzer.[22]

The analytical procedure outlined above was used to profile the $Al_xGa_{1-x}As$ layers obtained by the melt-mixing LPE technique. Figure 18(a) shows the As measured 400 KeV proton backscattering yield curve on a graded AlGaAs layer on a GaAs substrate obtained using a multi-channel analyzer and 2 KeV channel separation. The data in Fig. 18(b) has been treated by a simple graphical procedure in order to approximately correct for the detector resolution of ∿8 KeV. The linear extrapolation of the GaAs background spectra is also shown.

Fig. 19 shows the result obtained for the spectrum shown in Fig. 18. This particular growth was obtained using the melt-drop technique using only one drop. It shows that the graded region extends to only about 0.15μm near the interface. From our earlier estimates using SEM and Sputter-Auger Electron analyses we expected this region to be about 0.3μm.

Fig. 20 shows the result obtained on another graded bandgap GaAlAs layer grown using the chimney and funnel type melt-mixing setup described in section 3.1). It shows a graded region which is extending to about 0.3μm region near the interface. This is also shorter than our earlier estimates of about 0.5μm graded region. These results demonstrate the capability of this back-

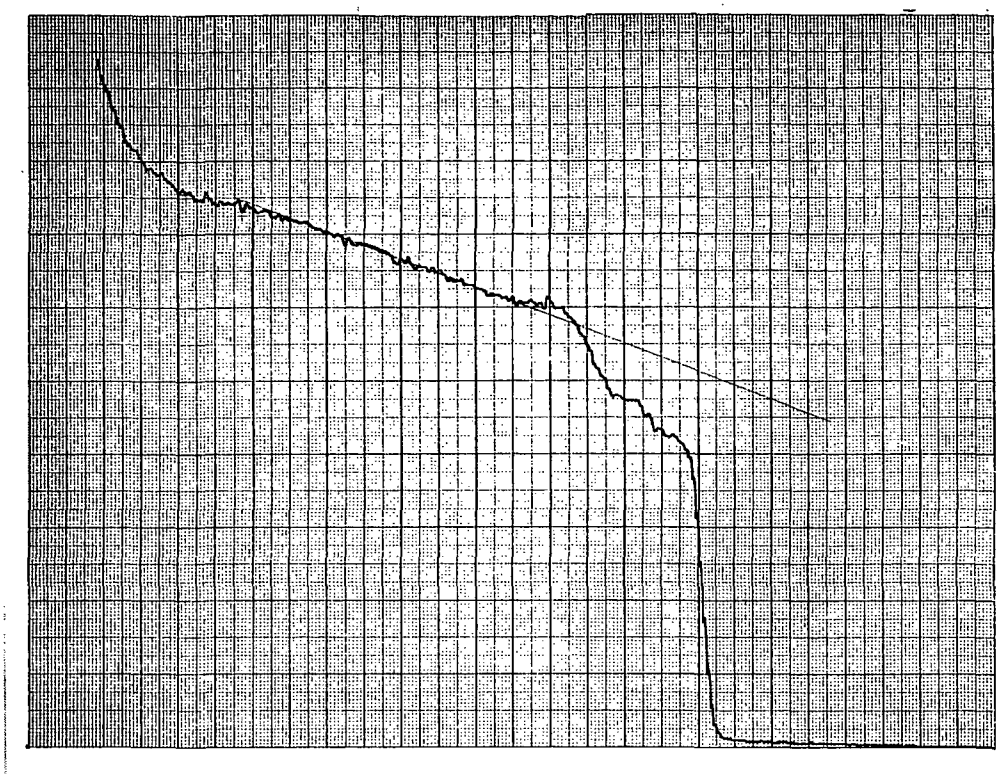

(a)

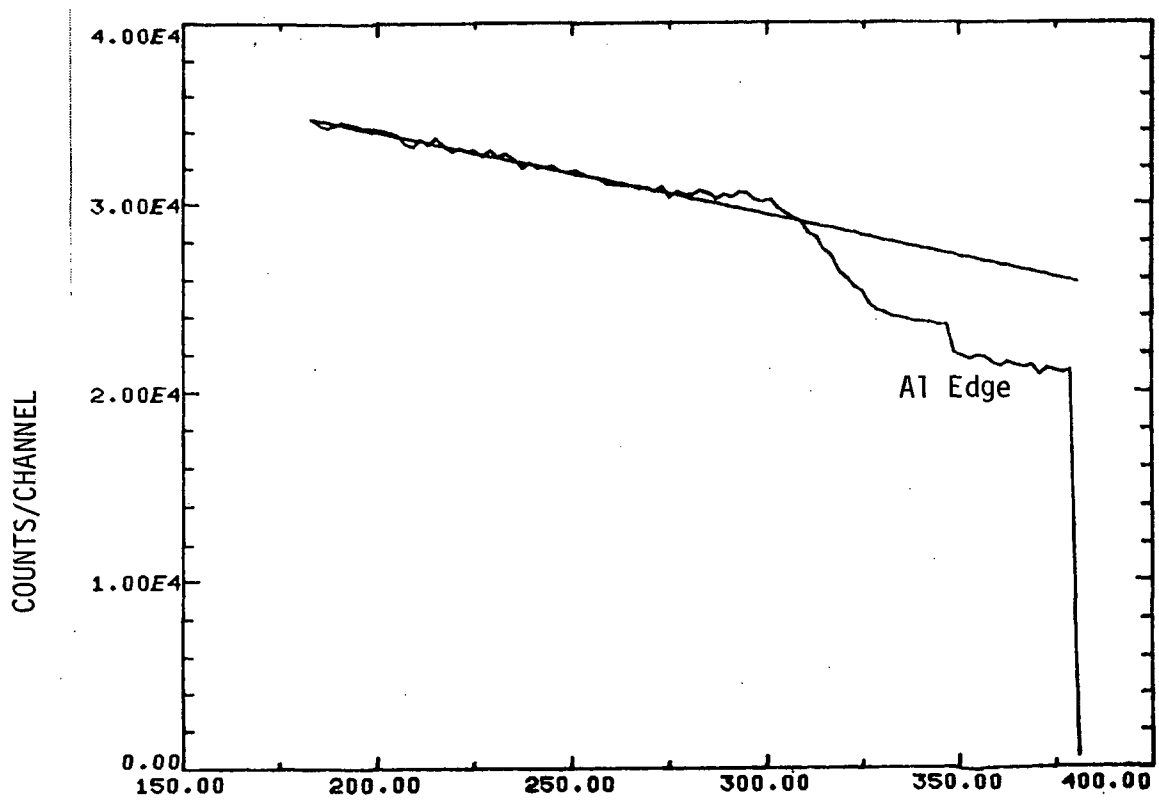

(b)

Fig. 18 (a) Experimentally measured 400 keV proton backscattering yield curve on a graded AlGaAs layer on a GaAs substrate.

(b) Above spectra corrected for the detector resolution. It also shows the linear extrapolation of the GaAs background spectra.

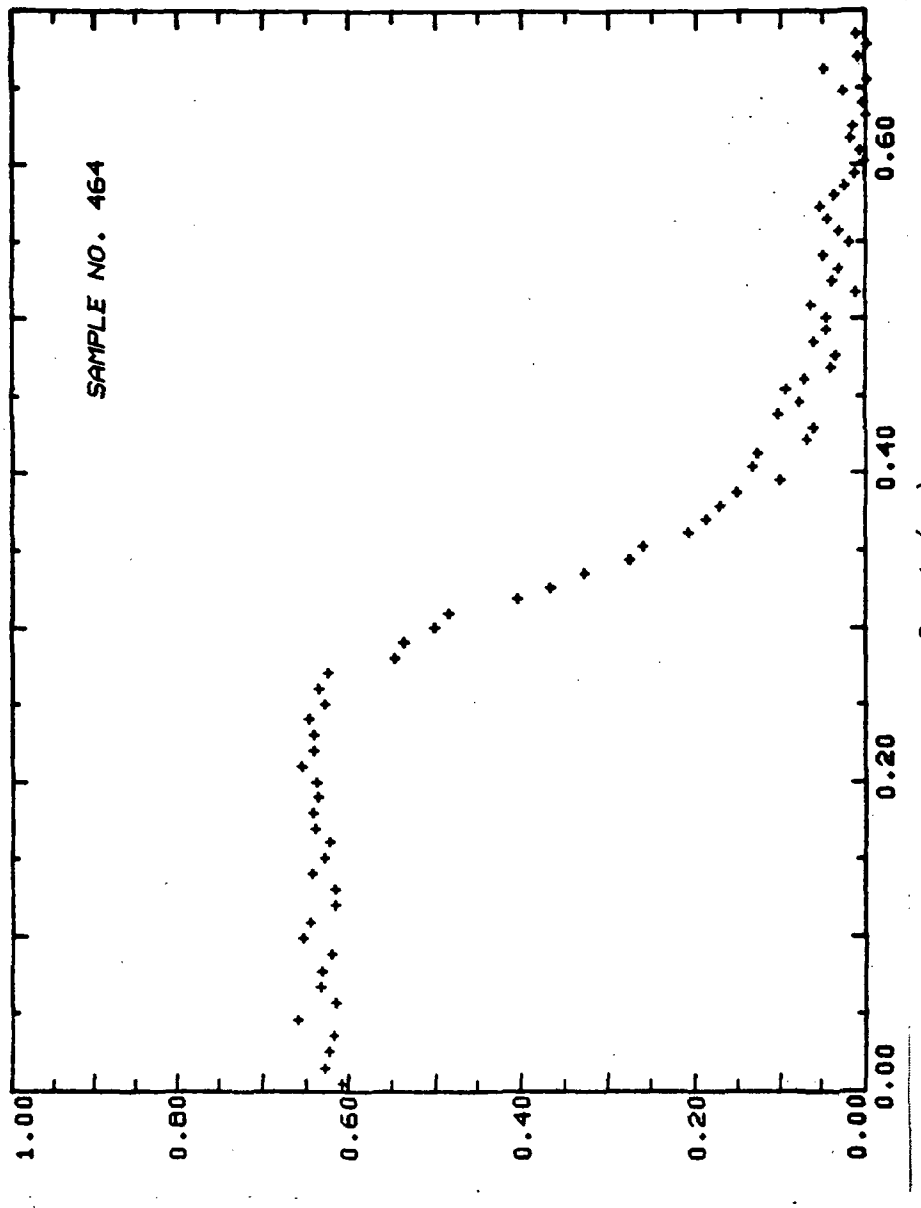

Fig. 19 Composition profile obtained from the backscattering data on a graded GaAlAs layer.

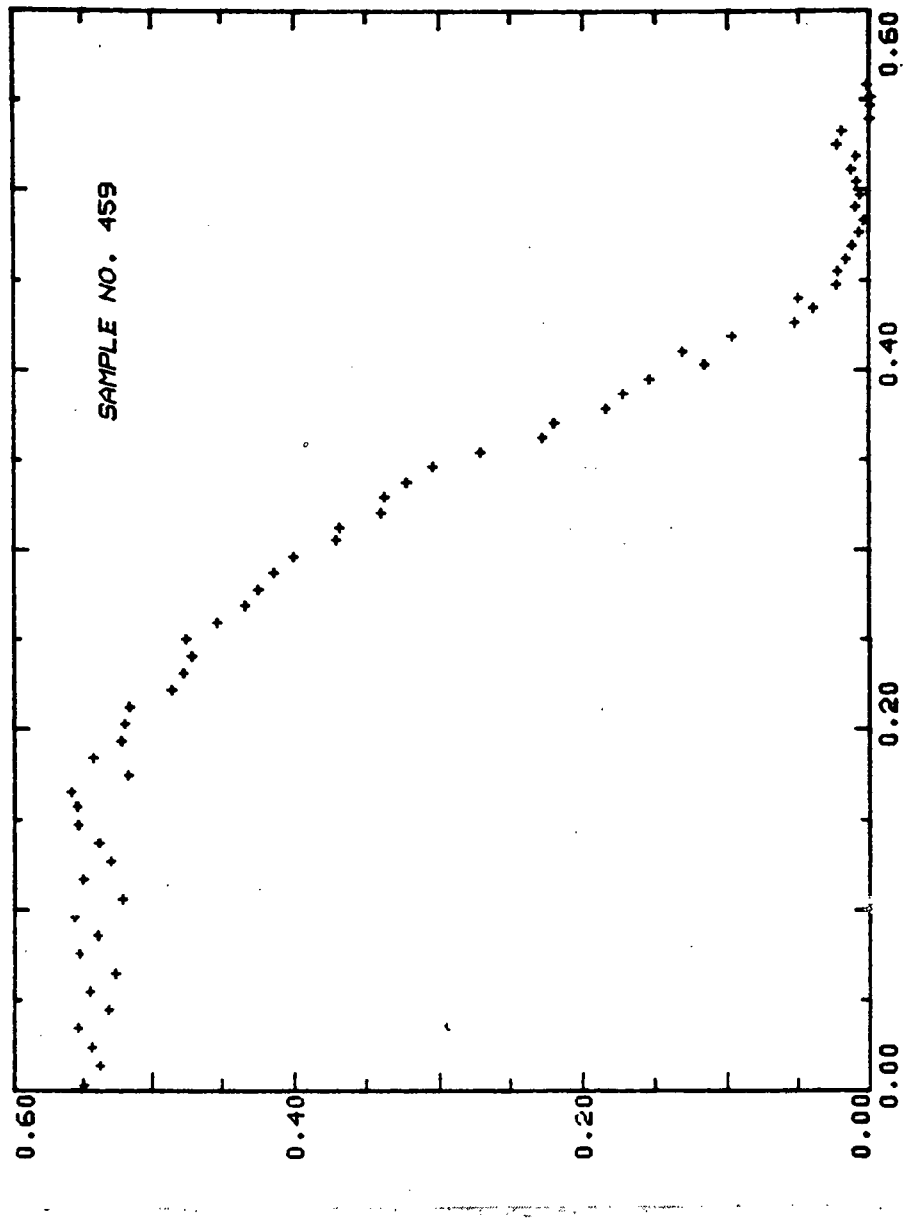

Fig. 20 Composition profile obtained from the backscattering data on a graded GaAlAs layer.

scattering analysis technique to analyze GaAlAs LPE layers as thin as 1500Å.

3.2.4 Sputter-Auger Profiling

We also used the Sputter-Auger electron analysis technique for depth profiling. The experimental set-up at our facility sputters about 1 mm diameter area and the Auger electron analysis is performed at the center of the sputter etched area. However, the sputter etched area obtained by this technique does not result in a good flat bottom and therefore errors are introduced due to roughness and non-linear etching rate at the analysis site. We sent some of our graded bandgap solar cell growths to Professor Spicer at Stanford University[23] for profiling using their Auger analysis system where the depth profile is obtained by analyzing the center of a raster scanned sputter etched area. Figure 21 shows the qualitative result obtained on a graded GaAlAs layer. It shows a rather strange profile with a steeply graded region at the interface followed by a dip in the Al concentration and then an extensive region with constant composition out to the front surface. Similar strange features with local regions of enhanced or depleted Al concentration were observed in other samples. The constant composition region at the surface indicates that the melt has reached equilibrium during the growth period (typically <60 sec). In order for the melt to reach equilibrium by diffusion the diffusion coefficient for Al in liquid Ga would have to be $\sim 10^{-2} cm^2/sec$ which is about 3 orders of magnitude higher than the diffusion coefficients for other elements in Ga melts. These profiles are the basis of our belief that the melt mixing is mechanical rather than diffusion.

This Auger electron analysis technique combined with raster scanned sputter etching and suitable known composition standards, proved to be most sensitive technique to bring out the details of the composition profile. However, this technique is destructive in nature. The back-scattering analysis described earlier was found to be a useful nondestructive technique.

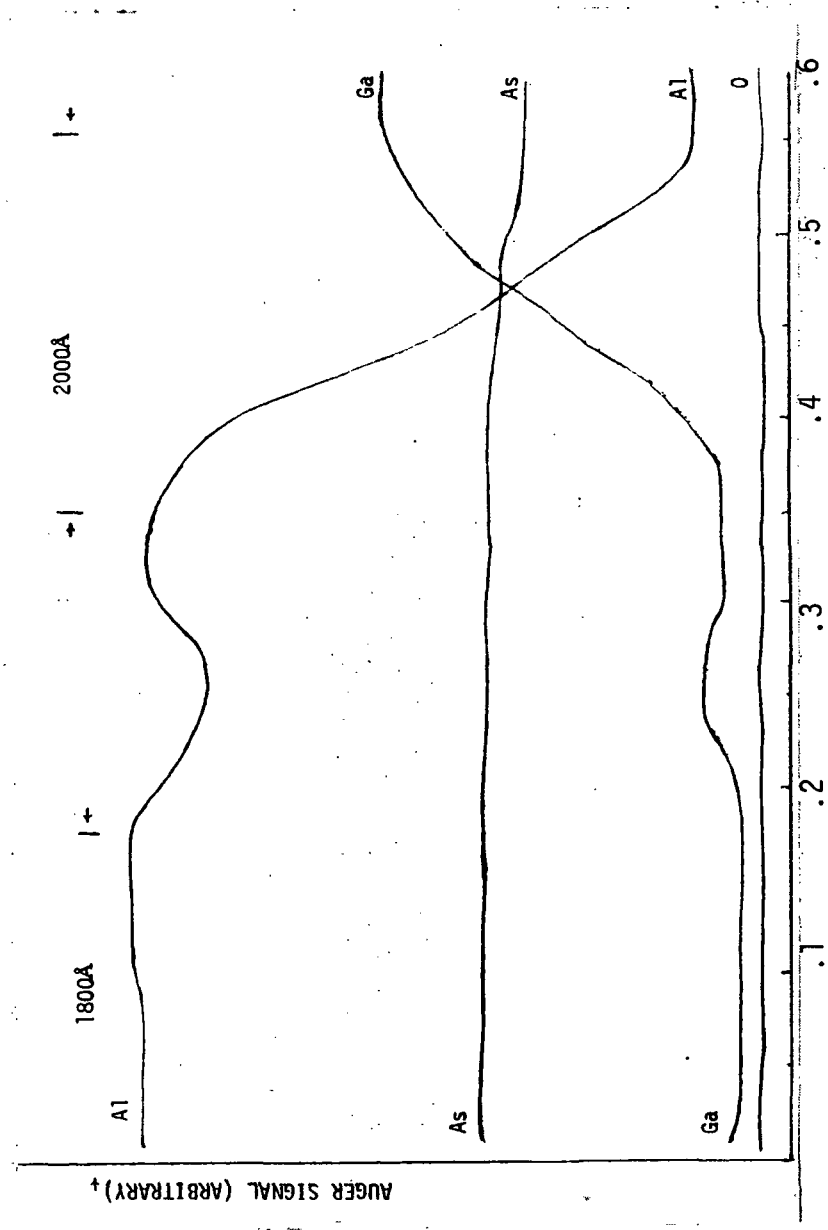

Fig. 21 Auger signals for Ga, Al and As for the graded GaAlAs layer as a function of sputtering time.

3.3 DEVICE FABRICATION

The test devices for the graded bandgap solar cell performance evaluation were fabricated from the LPE grown layers using the standard photolithographic and vacuum evaporation techniques. The sequence for the fabrication procedure for p/n type cells was as follows:

(1) Vacuum evaporation of Au-Ge/Pt ohmic contact on the substrate side

(2) Vacuum evaporation of Ag-Mn/Au ohmic contact on the front side through a bimetal mask

(3) Sintering of the ohmic contacts at 450°C for 4 minutes in the H_2 atmosphere

(4) Photolithographic technique to define the active area (65 x 65 $mils^2$) of the cell followed by mesa etching in Br-Methanol.

(5) Mounting the individual cell chips (75 x 75 $mils^2$) on a TO-5 header using silver epoxy and bonding gold wires to the front contact pads.

(6) Vacuum deposition of a Ta_2O_5 anti-reflection coating on the mounted devices

Fig. 22 shows the photograph of a test cell before the contact bonding. The front contact has six fingers, a central strip joining them with two contact pads. The contact area is only 6% of the total cell area.

The anti-reflection coating for these graded bandgap solar cells constitute an important fabrication step. We have an ongoing internally funded Independent Research & Development project (#843) for the development of high efficiency GaAlAs/GaAs heteroface solar cells. In that program, we have developed a computer model to calculate the optimum layer thicknesses for a single layer or a broadband double layer AR-coating based on the solar spectrum, the solar cell's internal photoresponse and the cell reflectivity. For the graded bandgap cells, we used only a single layer AR-coating. In Fig. 23, curve (a) shows the typical reflectivity vs. wavelength for a GaAlAs/GaAs graded bandgap solar cell. The curve (b)

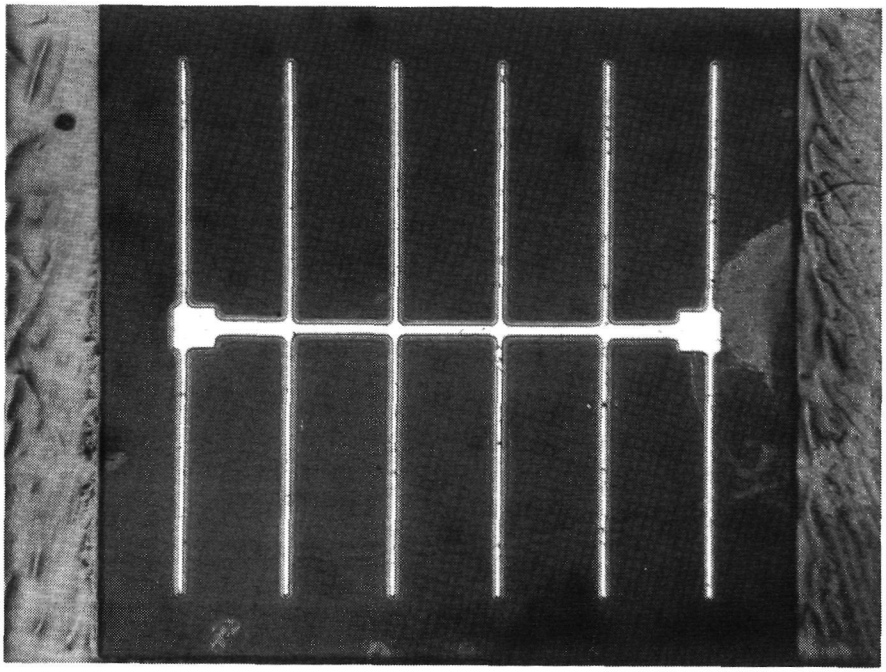

Fig. 22 Photograph of a finished test cell before contact bonding.

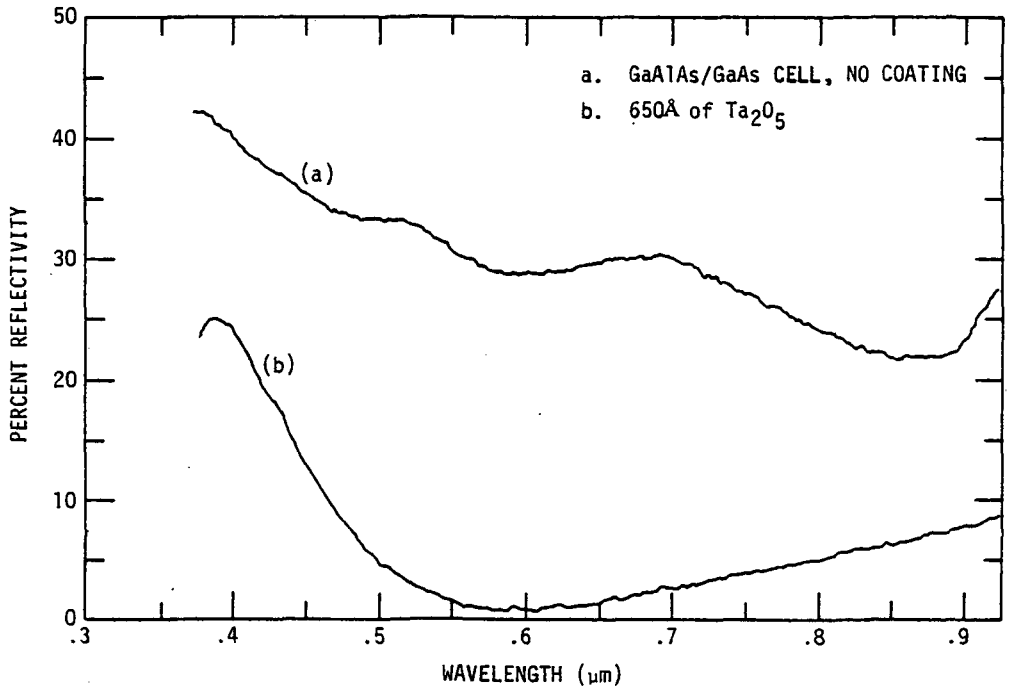

Fig. 23 The measured reflectivity of a GaAlAs/GaAs cell (a) without any AR-coating (b) with a single layer of Ta_2O_5 about 650Å thick.

shows the result of depositing 650Å of Ta_2O_5 on this cell. Here the net reflection loss is lowered from ~30% to less than 7%.

3.4 EFFICIENCY MEASUREMENTS

The highest efficiency we measured for an AR coated graded bandgap n/p solar cell under AMO illumination was 13.6%. The cell size was 65 mil square and the contact area was ~6% of the total area. The spectral response of this cell, #468A, is shown in Fig. 5. The measured J_{sc} using a Spectrolab AMO solar simulator at Rockwell Space Division was 24.4 ma/cm^2, V_{oc} = 0.88 V, and fill factor 0.76. We found that the efficiency could be increased to 15+% by etching the cell slightly to remove the ungraded GaAlAs near the surface. This improvement resulted solely from an increase in J_{sc}.

Most of the n/p cells we measured had 12-13.5% efficiency. These low efficiencies are due to low values for V_{oc} and the fill factor in addition to lower than expected J_{sc}. Although we do not have any AMO efficiency measurements to report for our p/n graded bandgap cells, it is instructive to make a comparison of V_{oc} and fill factor for our n/p cells vs. Zn-doped p/n cells. This is shown in Table I.

It was found that p/n cells have significantly larger maximum and typical values of both V_{oc} and fill factor than do n/p cells. These numbers mean that, in general, we can expect a p/n cell to have ~4% greater efficiency than a n/p cell if the short circuit currents are equal. Since this is usually true for optimized structures grown in a similar manner, it is clear than p/n cells will result in the highest efficiencies.

The use of Zn as the p-type dopant results in the higher V_{oc} and fill factor values for p/n cells. Zn begins to dfifuse easily in GaAs when the doping level is larger than 1 x 10^{18}cm^{-3}. During the period before growth when the system is hot, the high vapor pressure of Zn causes almost half of the Zn in the GaAlAs melt to evaporate. Some of this Zn is deposited on the uncovered substrate and is free to diffuse in. Also, Zn is free to diffuse further into the substrate during the ~10 min growth period of the Zn-doped p-GaAs layer. These two considerations result in

TABLE I

Comparison of n/p and p/n cells

	n/p cells	p/n cells
V_{oc}	1. Maximum 0.90 V 2. Typical $V_{oc} \sim 0.80$ V with large variation from cell to cell.	1. Maximum 0.99 V 2. Typical $V_{oc} \sim 0.95$ V with smaller variation from cell to cell.
Fill Factor (F.F.)	1. Maximum 0.78 2. Typical F.F. $\sim$0.70	1. Maximum 0.86 2. Typical F.F. $\sim$0.80

the p-n junction formation within the substrate ~1000Å away from the metallurgical interface. The depletion reigon of the cell is therefore away from the usual growth defects at the metallurgical interface. This results in less excess diode current which is responsible for the higher V_{oc} and fill factor values. In support of this, p/n cells we have made using Be or Ge as the p-type dopants do not show any higher values of V_{oc} and fill factor in general than our n/p cells.

4.0 CONCLUSIONS AND RECOMMENDATIONS

In this program we have demonstrated that an Al gradient in the $Ga_{1-x}Al_xAs$ surface layer of the GaAlAs/GaAs solar cell does help in the collection of current carriers generated near the surface if the built-in electric field extends up to the surface. The LPE process used to fabricate such structures is, however, unable to achieve the desired grading up to the surface in a reproducible manner because of the uncontrollable melt mixing process which results in a shorter than desired grading length that is not monotonically increasing out to the surface and spatial non-uniformities. Therefore, it can be concluded that the LPE process does not lend itself well to the growth of relatively thick (>0.5μm) graded $Ga_{1-x}Al_xAs$ layers over large area substrates (>0.5 cm^2). As discussed in the approach section, the LPE process utilizing a melt-mixing technique looked promising at the beginning of this program because the technique was capable of producing the high quality GaAs epitaxial materials required for solar cells. Looking at the progress made in the Molecular Beam Epitaxy (MBE) technology in the recent year, this now looks like the best candidate for fabricating these high efficiency graded band-gap GaAlAs/GaAs solar cells. This new technology is inherently capable of providing very uniform large area growths with sufficient control over the composition grading.

The Rutherford backscattering analysis technique was developed during this program to obtain the composition vs. depth profile of the $Ga_{1-x}Al_xAs$ surface layer. This non-destructive technique can be used to analyze ∿1μm thick layers using 500 KeV protons. The accuracy near the surface is, however, limited by the detector resolution. For thinner films and also to analyze the near surface region, the Sputtering-Auger Electron analysis technique can provide very good composition profiles.

The other conclusion drawn during the course of this program is the superiority of Zn-doped p on n cells over the n on p cells. This results from the high diffusion coefficient of Zn into GaAs at the doping concentration levels used for solar cells (∿$10^{18}cm^{-3}$) as compared to the

n-type dopants Sn and Te. The formation of a diffused p-n junction rather than a grown p-n junction results in better junction characteristics and uniformity. Therefore, it is recommended that further work on such graded bandgap GaAlAs/GaAs solar cells be devoted to Zn-doped p on n cells by the MBE technique.

5.0 REFERENCES

1. "Solar Cells, Outlook for Improved Efficiency," National Academy of Sciences, 1972.

2. J.J. Loferski, J. Appl. Phys. 27, 777 (1956).

3. J.A. Hutchby, Appl. Phys. Lett. 26, 457 (1975).

4. R. Sahai and A.G. Milnes, "Heterojunction Solar Cell Calculations," Solid State Electronics 13, 1289 (1970).

5. B. Ellis and T.S. Moss, "Calculated Efficiencies of Practical GaAs and Si Solar Cells Including the Effect of Built-In Electric Fields," Solid State Electronics 13, 1 (1970).

6. S.C. Tsaur, A.G. Milnes, R. Sahai and D.L. Feucht, "Theoretical and Experimental Results for GaAs Solar Cells," Proc. of 1972 Symposium on GaAs, 156(1972).

7. K.V. Vaidyanathan and G.H. Walker, "The Effect of Be^+ Ion Implanted Exponential and Uniform Impurity Profiles on the Electrical Characteristics of GaAs Solar Cells," 10th Photovoltaic Specialists Conference, 1973.

8. H.J. Hovel and J.M. Woodall, "Theoretical and Experimental Evaluations of $Ga_{1-x}Al_xAs$-GaAs Solar Cells," 10th Photovoltaic Specialists Conference, 1973.

9. J.A. Hutchby, Conf. Rec. of 1975 Photovoltaic Specialists Conference held at Scottsdale, Arizona, p. 416 (1975).

10. J.A. Hutchby and R.L. Fudurich, J. Appl. Phys. 47, 3140(1976).

11. J.A. Hutchby and R.L. Fudurich, J. Appl. Phys. 47, 3152 (1976).

12. J.F. Black and S.M. Ku, "Preparation and Properties of AlAs-GaAs Mixed Crystals," J. Electrochem. Soc. 113, 249 (1966).

13. M.B. Panish, I. Hayashi and S. Sumski, "A Technique for the Preparation of Low-Threshold Room-Temperature GaAs Laser Diode Structures," IEEE Journal of Quantum Electronics 5, 210 (1969).

14. H. M. Manasevit, "The Use of Metal-Organics in the Preparation of Semiconductor Materials," J. Electrochem. Soc. 118, 647 (1971).

15. M. B. Panish and S. Sumski, "Ga-Al-As Phase, Thermodynamic and Optical Properties," J. Phys. Chem. Solids, 30, 129 (1969).

16. J. S. Harris, Jr. and R. Sahai, "1.06 Micron High Sensitivity IR Photocathode," Technical Report AFAL-TR-74-68, 1974.

17. W. F. Hall et al., "Non-Destructive Determination of Energy-Gap Grading in Thin Film by Optical Transmission Measurements," Proceedings of the 3rd Annual Conference on the Physics of Compound Semiconductor Interfaces held at NELC, San Diego (1976).

18. James A. Hutchby, "High Efficiency Graded Bandgap $Al_xGa_{1-x}As$-GaAs p on n Solar Cell," Proc. of the Eleventh IEEE Photovoltaic Specialists Conference, p. 414 (1975).

19. W. K. Chu et al., "Principles and Applications of Ion Beam Techniques for the Analysis of Solids and Thin Films," Thin Solid Films, 17, 1 (1973).

20. L. C. Northcliffe and R. F. Schilling, Nuclear Data Tables A7, 233 (1970).

21. K. Gamo et al., Proc II Int'l Conf. on Ion Beam Surface Layer Analysis, Karlsruhe, Germany (1975).

22. R. Behrisch and B. M. V. Scherger, "Rutherford Backscattering as a Tool to Determine Electronic Stopping Power in Solids," Thin Solid Films, 19, 247 (1973).

23. C. M. Garner et al., "Auger Depth Profiling of Au-AlGaAs Interfaces and LPE AlGaAs-GaAs Heterojunctions," to be published in the Proc. of the 4th Conf. on Interfaces of Compound Semiconductors, Princeton, N.J. (Feb. 1977).